AFCRL-62-141

GENERAL ELECTRIC

Research Laboratory

SCHENECTADY, N.Y.

INVESTIGATION OF SEMICONDUCTING PROPERTIES OF II-VI COMPOUNDS

M. Aven and H.H. Woodbury

Scientific Report No. 2

Contract No. AF19(604)-8512
Project 4608
Task 46088

Period Covered: November 1, 1961 - February 1, 1962

Prepared

for

ELECTRONICS RESEARCH DIRECTORATE
AIR FORCE CAMBRIDGE RESEARCH LABORATORIES
OFFICE OF AEROSPACE RESEARCH
UNITED STATES AIR FORCE
BEDFORD, MASSACHUSETTS

AFCRL-62-141

INVESTIGATION OF SEMICONDUCTING PROPERTIES OF II-VI COMPOUNDS

M. Aven and H. H Woodbury
General Electric Research Laboratory
Schenectady, N. Y.

Scientific Report No. 2
for Period Nov. 1, 1961 - February 1, 1962
Contract No. AF19(604)-8512
Project 4608 Task 46088

Prepared for
Electronics Research Directorate
Air Force Cambridge Research Laboratories
Office of Aerospace Research
United States Air Force
Bedford, Massachusetts

Requests for additional copies by Agencies of the Department of Defense, their contractors, and other Government agencies should be directed to the:

ARMED SERVICES TECHNICAL INFORMATION AGENCY
ARLINGTON HALL STATION
ARLINGTON 12, VIRGINIA

Department of Defense contractors must be established for ASTIA services or have their "need-to-know" certified by the cognizant military agency of their project or contract.

All other persons and organizations should apply to the:

U.S. DEPARTMENT OF COMMERCE
OFFICE OF TECHNICAL SERVICES
WASHINGTON 25, D.C.

TABLE OF CONTENTS

ABSTRACT

Experiments with heavily Cu-doped CdS ~~have established that~~ this material contains a second phase which can be readily observed and ~~which has been seen to~~ decorates crystalline imperfections. ~~The connected character of these precipitates suggests the presence of conducting paths through crystals doped with~~ high concentrations ~~of Cu and showing p-type conductivity~~. Consideration is given to the possible positions of the thermal acceptor levels for Cu, Ag and Au in CdS ~~in relation to~~ with the objective of preparing p-type CdS ~~which will not contain~~ without precipitates of a second phase.

Hall effect measurements on n-type ZnSe and p-type ZnTe ~~have~~ were ~~been~~ made; ~~and~~ the resulting mobility-temperature relationships ~~have been~~ were compared to theoretical estimates. The measurements ~~have also~~ yielded tentative positions for donor levels in ZnSe and acceptor levels in ZnTe.

ZnTe-CdS heterojunctions ~~have been~~ were prepared ~~which show~~ with current-voltage characteristics indicative of p-i-n or p-n*-n type junction structure. Examination of cross-sections of such junctions ~~has~~ revealed ~~the presence of~~ a layer which is presumably intrinsic or very weakly n-type.

1. INTRODUCTION

The broad objective of the work to be described below has been to evaluate the feasibility of using wide band gap II-VI compounds as components of semiconductor devices. The difficulty in preparing II-VI compounds in both conductivity types is well known. The task has, therefore, been to find ways to prepare these compounds in the conductivity types which have, up until now, resisted synthesis, or to devise means to prepare junctions of two different II-VI compounds.

In the area of trying to synthesize a particular II-VI compound in both conductivity types, the main attention has been focussed on preparing p-type CdS, as n-type CdS is known to have good semiconductor properties. Section 2 of this report will describe the micro-structure of heavily Cu-doped CdS which has been assumed to represent true one-phase p-type CdS by some workers. The presented evidence will show that, in all probability, this has been a two-phase system in which the conduction paths are made up of interconnected precipitates. Preliminary experiments designed to render Ag-activated CdS p-type will also be discussed in this section.

It was described in Scientific Report No. 1 how a novel firing technique had led to the synthesis of moderately low resistivity n-type ZnSe. Further work with this compound has now made it possible to prepare it with a room temperature electron mobility

of 530 cm^2/volt sec, which is one of the highest mobilities reported for compounds of comparable band width and degree of polar character. Hall effect measurements with n-type ZnSe will be presented in Section 3.1 along with theoretical estimates of the mobility-limiting scattering mechanisms in this compound. Section 3.2 will be devoted to a similar treatment of p-type ZnTe. In the two following sections tentative positions of donor levels in n-type ZnSe and acceptor levels p-type ZnTe will be deduced from the temperature dependence of the Hall coefficient.

Section 4 will cover the area of ZnTe-CdS heterojunctions. Changes in junction design parameters will be described which have led to significantly improved current-voltage characteristics in the forward bias region. It will also be shown how different fluorescent response under ultraviolet irradiation has made it possible to distinguish between an intrinsic or weakly n-type layer and a more strongly n-type layer in the CdS films deposited on ZnTe crystals. Photomicrographs of CdS films on differently oriented portions of ZnTe crystals will illustrate some of the growth habits of CdS.

2. CADMIUM SULFIDE

The effort to produce p-type CdS has so far failed. The main emphasis has been on doping CdS with Cu, Ag, and Au, although preliminary experiments with other possible dopants have been tried (see previous status report). In the work with Cu, Ag, and Au, two principal difficulties have been apparent. One difficulty is keeping the impurities in solution at high concentration; the second is the apparent depth of the acceptor level. These difficulties are discussed below.

Previous workers[1] have found that when CdS is doped to concentrations of greater than 10^{-2} mole percent of uncompensated Ag or Cu, grey products result indicating precipitation. We have also observed this. In particular, attempts to produce very heavily Cu-doped crystals led to samples showing visible structure under ordinary microscopic studies. Fig. 1 shows two examples of such structure. These are photographs taken with transmitted light through thin (<10 mils) sections. Fig. 1A is of a crystal fired in an H_2S stream at 1000°C in a CdS powder containing 10 mole percent of Cu. Analysis showed that the average total Cu content of the crystal to be 4%. Fig. 1B is of a crystal also fired in an H_2S stream at 1000°C but in a powder doped to 1% Cu. The average Cu content of the crystal was 0.5%.

The pertinent point relating to the objectives of the contract is the connected character of the structure at these high

concentrations indicating possible conducting paths. The crystal containing 4 mole percent copper (Fig. 1A) showed p-type conductivity; the crystal containing 0.5 mole percent copper (Fig. 1B) showed very high resistivity.

Of greater significance, however, are the patterns indicating the decoration of grain boundaries and dislocations. Examination of the sample shown in Fig. 1B under higher power indicated that the "wiggly-line" structure is probably decorated dislocations. The "broad clear" regions in Figs. 1A and 1B are where Cu has been depleted byprecipitation along what are probably grain boundaries.

Concerning the second point relating to what might be expected about the position of the acceptor levels, we have considered the following: If one interprets the long wavelength emission band[2] as arising from a transition from the conduction band to the neutral activator level, one obtains a level model shown in Fig. 2. Because the broadening of these transitions involve considerable (unresolved) phonon structure, one expects the "thermal level" to correspond to the high energy edge of the emission bands. While no attempt has been made to analyze each emission curve, a brief inspection indicates the edge to be of the order of 0.25 ev (at 77°K) from the center position. On the basis of these assumptions and interpretations, the thermal acceptor energy for Au, Cu, and Ag would be approximately as indicated in Fig. 2. The conclusion is apparent: Ag is the most promising impurity of the three to

generate p-type conductivity but even it is so deep that "low-resistivity" material ($\rho < 10^6$ ohm-cm) is not normally expected at room temperature. However, it is felt very worth while to continue a study of Ag-doped CdS to determine if p-type material can be made and if so to ascertain the hole mobility and other pertinent parameters.

In the samples studied so far, resistivities of the order of 10^8-10^9 ohm-cm at 125°C have been observed in both undoped and Ag-doped crystals. The expected intrinsic resistivity is of the order of 4×10^{10} ohm-cm. All Hall measurements that have been made indicate n-type conduction. The conclusion is that deep n-type levels (i.e., compensated acceptor levels or donor levels situated above the middle of the band gap) are dominating the electrical behavior in these samples. These levels appear to be 0.8 - 1.1 ev from the conduction band. It is hoped that further study will lead to an understanding of these levels and how to lower the Fermi level below them (towards p-type behavior).

3. TRANSPORT PROPERTIES AND ENERGY LEVEL STRUCTURE IN ZnSe and ZnTe

3.1 Mobility Studies on n-type ZnSe

Recent work by Aven, Marple, and Segall[3] with ZnSe has indicated that the effective mass of the electrons in this compound lies between 0.1 m_o and 0.15 m_o. The quoted work also established the energy of the longitudinal optical phonon and the values for the static and high frequency dielectric constants.

With this information it is possible to calculate the electron mobility as limited by polar scattering. Using the Howarth and Sondheimer[4] expression, the mobility

$$\mu = \frac{1}{2\alpha\omega_l}\,\frac{q}{m^*}\,\frac{8}{3\sqrt{\pi}}\,\frac{(e^Z-1)}{Z^{1/2}}\,\varkappa(Z), \qquad (1)$$

where

ω_l is the frequency of the longitudinal optical phonon,

q is the electronic charge, and

m^* is the effective mass of the charge carrier.

$Z = \hbar\omega_l/kT = h\omega_l/2\pi kT$

h is the Planck's constant,

k is the Boltzman constant, and

T is the temperature.

$\varkappa(Z)$ is a slowly varying function arising from the perturbation treatment of optical mode scattering, and α, the coupling constant, is given by

$$\alpha = q^2 \left(\frac{m^*}{2\hbar\omega_\ell}\right)^{1/2} \frac{1}{\hbar} \left(\frac{1}{\epsilon_\infty} - \frac{1}{\epsilon_o}\right), \qquad (2)$$

where ϵ_∞ is the high frequency dielectric constant and ϵ_o is the static dielectric constant.

Insertion of the required quantities in the above expression, and changing to practical units gives

$$\mu \left(\frac{cm^2}{volt\ sec}\right) = 24.6\ T^{1/2}\ (e^{360/T} - 1)\ \gamma\left(\frac{360}{T}\right).$$

The values for the function γ, which for the temperature range of interest for ZnSe varies between 0.6 and unity, can be found in Reference (5).

The dependence of mobility on temperature as calculated from the above equation is shown in Fig. 3 as the solid line. On the same graph are shown the mobility data for three ZnSe crystals. ZnSe 4 was an undoped crystal, fired for 16 hours in liquid Zn at 1000°C. ZnSe 3 and ZnSe 5 were crystals doped with Cl which acts as a donor in II-VI compounds. ZnSe 5 was fired once, and ZnSe 3 twice at 1000°C in liquid Zn for periods of 16 hours.

It can be seen that the room temperature mobility of ZnSe 3 comes to within approximately 15 per cent of the mobility calculated assuming polar scattering to be the mobility limiting mechanism. The experimental curve, however, departs considerably from the theoretical, both below and above room temperature. It is reasonable to assume that the departure below room temperature is

caused by the onset of impurity scattering. This is probably also the reason why the mobility curves for ZnSe 4 and ZnSe 5 fall farther below the theoretical mobility curve even at room temperature. The reason for the deviations at higher temperatures is not clear as yet. Estimates have shown that the piezoelectric and the acoustical mode scattering is negligible in this temperature range. However, as several other II-VI compounds show similar deviations, it is suggestive that the theoretical expression for optical scattering may not correctly represent the change of mobility with temperature in this temperature range.

3.2 Mobility Studies on p-type ZnTe

It was mentioned in the preceding section that, in order to estimate the contribution to scattering of charge carriers by optical modes, it is necessary to know the values the static and the high frequency dielectric constants, the energy of the longitudinal optical phonon, as well as the effective mass of the charge carriers. For ZnTe, Shiozawa, Jost, and Devlin[6] have established values for all of these quantities except the effective mass. Preliminary curve fitting of the theoretical expression to some experimental data showed that an effective hole mass of the order of 0.6 m_o would bring the experimental and theoretical curves to near coincidence at room temperature. Since an effective hole mass of 0.6 m_o does not appear to be excessively large for ZnTe, it was inserted into the Howarth-Sondheimer expression as given by

Equation (1) in Section 3.1. This yielded the equation

$$\mu_{opt} = 8.04\ T^{1/2}\ (e^{302/T}-1)\ \chi\ (\frac{302}{T})$$

for the functional relationship between mobility and temperature. Fig. 4 shows a log-log plot of this equation along with the experimental measurements on some ZnTe crystals. ZnTe 126 is a crystal fired for 16 hours at 900°C in liquid Zn to remove impurities extractable by this technique. ZnTe 128 is a crystal first fired at 900°C in liquid Zn and then at 800°C in Te vapor. As in the case of ZnSe, the experimental mobility figures depart from the theoretical curve at both high and low temperatures. Again, it is fairly certain that the departure at low temperatures is due to impurity scattering, while at high temperatures the reason for the deviation is, as yet, unknown. There is, however, an additional complication which was not present with ZnSe. Because of the three valence bands, two of which are degenerate at k = 0 in ZnTe, one cannot overlook the possibility of interband scattering. Thus the figure of 0.6 m_o can at present be regarded at best as the upper limit for the effective mass of holes in ZnTe.

3.3 Donor Levels in ZnSe

There are very few references as to the position of the donor levels in ZnSe. In a table of donor and acceptor ionization energies for II-VI compounds, Bube and Lind[7] give 0.21 ev for

the donor level introduced by Br into ZnSe. The same authors have also observed that in the Zn compounds the donor ionization energies tend to be around 0.25 ev, while the donor ionization energies in CdS are much smaller - around 0.03 ev.

This finding, although well substantiated by several types of measurements such as glow curves, conductivity, etc., has been difficult to understand. Assuming the hydrogenic model to be valid, the relationship between the donor level, E_D, and the effective mass of electrons, m^*, is given by [8]

$$m^* = \frac{h^2 \epsilon_o^2 E_D}{2\pi^2 q^4} \qquad (3)$$

Using the donor ionization energy of 0.03 ev, Eq. 3 gives approximately 0.2 m_o as the effective mass of electrons in CdS, which figure agrees well with effective mass determination from mobility[9] and free carrier absorption[10] measurements. A similar calculation for ZnSe, using a donor ionization energy of 0.2 ev, would lead to an effective electron mass of approximately 1 m_o which is considerably higher than the measured value[3] of 0.1 to 0.15 m_o (the activation energy corresponding to an effective mass of 0.15 m_o is 0.03 ev). As there is little doubt about the existence of the 0.2 ev level in ZnSe, one concludes that this level, like many deep donor and acceptor levels in semiconductors, is not hydrogenic. This poses the question of

why CdS exhibits hydrogen-like donor levels, while ZnSe, a compound very similar to CdS, does not.

A possible answer to this can be derived from the fact that the measurements yielding the 0.2 ev donor level for ZnSe have been carried out with insulating or weakly n-type ZnSe crystals. Thus, any shallow hydrogenic levels were probably compensated. If this assumption is correct, one should find these levels in more strongly n-type ZnSe.

The data in Figs. 5 and 6 shows a trend towards shallower levels with the increase in carrier concentration. ZnSe 3, a crystal doped with approximately 10^{19} cm^{-3} Cl and fired at 1000°C in liquid Zn, has a room temperature free carrier concentration of about 2×10^{15} cm^{-3}. As the donor concentration in this crystal is about four orders of magnitude higher than the free electron concentration, and the donor ionization energy is not particularly large, it can be assumed that this crystal is compensated to a high degree by acceptor impurities. Under such conditions, and if $kT \ll E_D$, the free electron concentration, n, can be expressed as[11]

$$n = \left(\frac{2\pi m^* kT}{h^2}\right)^{3/2} \left(\frac{N_D - N_A}{N_A}\right) e^{-E_D/kT} \qquad (4)$$

where N_D is the donor and N_A is the acceptor concentration, the other symbols being identified before. Within the approximations noted above, the $T^{3/2}$ term is negligible in comparison with the

exponential term, and a simple plot of log R_H^* versus 1/T will yield $E_D/(2.3k)$ as its slope. The slope of 0.19 ev/(2.3k) in Fig. 5 thus indicates the presence of a 0.19 ev deep donor level. The closeness of this value to the donor ionization energy of 0.21 ev reported by Bube for bromine-doped ZnSe suggests that the donor centers in these materials are of identical nature.

Fig. 6 shows a similar plot for a ZnSe crystal identical with ZnSe 3 except for being fired twice in liquid Zn in order to extract more of the acceptor impurities (cf. next section) and thus reduce the degree of compensation. The Hall measurement data show that, as expected, the room temperature free carrier concentration in this crystal is about one order of magnitude higher than in ZnSe 3. The log R_H versus 1/T slope is 0.04 ev/2.3k. The data is not carried to sufficiently low temperatures to allow the approximations made in deriving Eq. 4 and therefore the donor ionization energy in this crystal should not be taken as 0.04 ev. Fig. 7 shows a plot of log R_H versus 1/T for ZnSe 4, an unactivated crystal

---

* The relationship between n and R_H is given by $n = -\frac{f}{R_H q}$, where f is a factor ranging between rougly 1 and 2 depending on the mechanism of scattering. As the exact scattering mechanism in ZnSe and ZnTe is not known, f = 1 will be used throughout this report for simplicity.

(i.e. a crystal which must have a low concentration of the 0.2 ev donor levels attributed to halogens) fired twice in molten Zn. In spite of appearing linear over a temperature range of more than 300 K^{o}, the apparent slope of 0.014 ev/2.3k again does not represent the true donor ionization energy, as the condition $E_D >> kT$ is not fulfilled over most of the covered temperature range.

In spite of the inability to extract a reliable donor ionization energy from the data in Figs. 6 and 7, it can be stated with certainty that the donor ionization energy in these crystals must be considerably below 0.2 ev. A very rough estimate, using only the extreme low temperature portion ($< 70°K$) of Fig. 7, gave an activation energy of the order of 0.01 ev which is not out of line with the hydrogenic level depth of 0.03 ev.

It is intended next to try to extend the Hall measurements on n-type ZnSe to lower temperatures to obtain a more accurate estimate for the donor ionization energy.

3.4 Acceptor Levels in ZnTe

The investigation of the acceptor level structure in ZnTe has had a two-fold objective. First, as the p-type component of a ZnTe-CdS heterojunction, ZnTe must have high p-type conductivity, preferably of the order of 10 to 100 $ohm^{-1}\ cm^{-1}$. Therefore one has to determine which of the possible acceptors will lead to the highest carrier concentration without adversely affecting the hole mobility. Second, as a possible material for p-n homojunction

devices, ZnTe has to be synthesized in n-type form. The failure to obtain ZnTe in n-type form to date has been ascribed to either the inability to remove traces of Cu, which acts as an acceptor in II-VI compounds or to spontaneous formation of native acceptor centers whenever one introduces foreign donor impurities. It has been suggested that Cu introduces acceptor levels at approximately 0.3 and 0.1 ev above the valence band edge.[7] The species as well as the position of the level of the native acceptor, however, is unknown. The knowledge of the acceptor level structure in ZnTe is, therefore, also a prerequisite for finding methods for synthesizing ZnTe in n-type form.

The most likely native acceptor center in ZnTe is the Zn vacancy. An interstitial Te, which has sometimes been suggested as a possible acceptor species, can probably be ruled out because of its very large ionic size and its repulsive potential for electrons, if present in an interstitial site. The tendency of ZnTe to form an excess of Zn over Te vacancies is not hard to understand in view of the greater volatility of Zn. Therefore ZnTe would be expected to act as a p-type semiconductor even without the presence of any foreign acceptor impurities. It will be shown below that, while in some cases Cu is present in "undoped" ZnTe crystals, ZnTe prepared with careful exclusion of Cu still contains a substantial concentration of acceptor centers. Fig. 8 shows a plot of log p, the hole concentration, against the 1/T

for ZnTe 117, a single crystal bar cut out of an undoped vapor-grown ZnTe boule. According to semiconductor theory, if $kT \ll E_A$, the hole concentration is given as[11]

$$p = \left(\frac{2\pi m^* kT}{h^2}\right)^{3/2} \left(\frac{N_A - N_D}{N_D}\right) e^{-E_A/kT} \tag{5}$$

if $p < N_D$ and $p \ll N_A - N_D$, and

$$p = \sqrt{2}\left(\frac{2\pi m^* kT}{h^2}\right)^{3/4} (N_A - N_D)^{1/2} e^{-E_A/2kT} \tag{6}$$

if $N_D < p \ll N_A - N_D$

where E_A is the acceptor ionization energy. As one starts warming up a semiconductor crystal in which there is very little compensation from low temperatures, one first meets the condition $p < N_D$, and therefore the ln p versus $\frac{1}{T}$ plot has a slope of E_A/k. As p increases with increasing temperature, eventually the condition $p > N_D$ is reached. In this temperature range the slope equals $E_A/2k$. At still higher temperatures all the holes will have been ionized out of the acceptor centers.

Fig. 8 clearly displays these three regions. At low temperatures the slope of the log p versus $\frac{1}{T}$ plot corresponds to an ionization energy of 0.166 ev (the term 2.3 in the denominator arises from converting natural to common logarithms). At intermediate temperatures the slope is approximately one half of the low temperature slope, and at still higher temperatures the curve

levels off at a carrier concentration of 2.3×10^{16} cm^{-3}. From this information it is possible to calculate the concentration of both the acceptors and donors in this sample by solving the following two simultaneous equations

$$\text{at } 166^\circ\text{K} \quad p = \left(\frac{2\pi m^* kT}{h^2}\right)^{3/2} \left(\frac{N_A - N_D}{N_D}\right) e^{-\frac{E_A}{kT}}$$

$$\text{at } 450^\circ\text{K} \quad p = N_A - N_D$$

Using 0.6 m_o for the effective mass (cf. Section 3.2), and inserting the experimentally determined values for n and E_A^*, gives

$$N_A = 1.9 \times 10^{16} \text{ cm}^{-3}$$

$$N_D = 3 \times 10^{15} \text{ cm}^{-3}$$

An internal check of this calculation is obtained by comparing the calculated donor concentration to the approximate position of the break in the log p versus $\frac{1}{T}$ plot where the E/2.3 k shope goes over to E/2(2.3k). At this point $n \tilde{\approx} N_D$. It can be seen in Fig. 8 that the break does occur near $n = 3 \times 10^{15}$ cm$^{-3} \tilde{\approx} N_D$, as required. This agreement shows that the effective mass of 0.6 m_o is not inconsistent with the Hall measurements in this crystal.

---

* Since this calculation depends critically on the exact value of E_A, the ionization energy used here was determined from a replot of Fig. 8, taking the $T^{3/2}$ variation of the density of states into consideration. The value thus obtained was slightly lower, namely 0.150 ev.

Fig. 9 shows a plot of log R_H versus $\frac{1}{T}$ for ZnTe 113, a crystal doped with approximately 10^{18} cm^{-3} Cu. The acceptor ionization energy in this crystal is 0.15 ev, which is close to the ionization energy found for the above discussed crystal ZnTe 117. It is suggestive, therefore, that the acceptor impurity in crystal ZnTe 117 is Cu. Indeed, when crystal ZnTe 117 was subjected to firing at 900°C in liquid Zn, which treatment presumably extracts some of the Cu impurity, a radical change in the slope of the log R_H vs $\frac{1}{T}$ plot was observed, as evidenced by Fig. 10.

The effect of the liquid Zn firing was tested with a number of other ZnTe crystals. It was found invariably that this treatment eliminated the 0.15 ev level found in Cu-contaminated crystals. In crystals which did not show the ~ 0.15 ev slope and thus presumably did not contain as much Cu impurity, the Zn treatment usually reduced the room temperature carrier concentration by approximately a factor of two.

Attempts to follow the Cu extraction by chemical analysis in relatively pure crystals was inconclusive, because of insufficient sensitivity of analytical techniques at concentrations below 10^{16} cm^{-3}. Using crystals containing of the order of 10^{18} cm^{-3} Cu, however, it has been established by chemical analysis that the liquid Zn treatment affords a reduction of Cu concentration by a factor of 2 to 3 (using a 2:1 Zn to ZnTe weight ratio).

It is therefore very likely, although admittedly not conclusively proven, that liquid Zn removes Cu also when it is present in lower concentrations.

The other conceivable effects of the Zn-firing is the removal of oxygen impurity and the reduction of the Zn vacancy concentration. Although these effects are undoubtedly present to some degree, it is believed that they are taking place concurrently with rather than instead of the Cu removal. Oxygen, being a divalent ion, is expected to substitute for Te, and thus be electrically inactive. The effect of the change in Zn vacancy concentration on the log R_H vs $\frac{1}{T}$ relationship is illustrated in Fig. 11. ZnTe 1262 is a crystal which was fired at 900°C in liquid Zn, while ZnTe 1287 and ZnTe 1286 were fired in Te vapor, the former at 700°C, the latter at 800°C. The partial pressure of Te, and therefore also the Zn vacancy concentration, is thus increasing in the order of ZnTe 1262 → ZnTe 1287 → ZnTe 1286. Since the compensating donor concentration is constant in all of these crystals and was found to be of the order of 10^{15} cm^{-3}, the increase in the Zn vacancy acceptor concentration must be reflected in the increase in free hole concentration. The data in Fig. 11 indicates that this is, indeed, what is happening. The Hall coefficient at all temperatures decreases in the order ZnTe 1262 → ZnTe 1287 → ZnTe 1286, which means that the free hole concentration increases in the same order. This finding suggests that the Zn vacancy levels

are reflected by the curves shown in the figure. The reason why these curves are S-shaped rather than straight is probably derived from the fact that the Zn vacancy can act as a double donor, and the state of occupancy of each of these depends on the position of the Fermi level. It is also possible that there are still some residual foreign acceptor impurities, which affect the shape of the log R_H vs $\frac{1}{T}$ plots, particularly at higher temperatures. As the average slope of the S-shaped curves is rather low, and the plots traverse only slightly more than one decade in log R_H, it is not permissible to neglect the $T^{3/2}$ term in comparison to the exponential term in Equation 5 in trying to evaluate the ionization energy of the Zn vacancy levels. A plot of (log $R_H T^{3/2}$) for ZnTe 1286, the crystal having the highest concentration of Zn vacancies, revealed a slope of 0.04/2.3 k at low temperatures ($T < 120°K$). At intermediate temperatures the curve almost leveled off, suggesting saturation. At the high temperature end ($T > 240°K$) there appeared a region of another steeper slope, indicating the presence of another acceptor level.

At the low temperature portion of this plot the condition $E_D \gg kT$ is not seriously violated, but the fact that here $p \tilde{\approx} N_D$ makes it difficult to decide whether Eq. 5 or 6 should be used in evaluating the acceptor ionization energy. In the former case $E_A = 0.04$ ev, and in the latter $E_A = 0.08$ ev. Although it is

tempting to pick the latter of these for the acceptor ionization energy, as E_A = 0.08 ev corresponds to an effective mass of 0.6 m_o, it is preferred not to make this identification at this time, pending confirmation by more extensive measurements.

4. ZnTe-CdS HETEROJUNCTIONS

Previous work with the ZnTe-CdS heterojunctions had established that a CdS film could be grown epitaxially on ZnTe single crystals if the substrate crystal was oriented so as to receive the CdS film on the (111) crystallographic face containing the Zn atoms. The work to be reported below has been concerned with the study of some crystallographic habits of the CdS film growth, the influence of the doping of the ZnTe substrate crystal on the electrical properties of the CdS film, and the rectifier characteristics of the heterojunction as a whole.

4.1 Crystallography

It was mentioned in Scientific Report No. 1 that the original identification of the polarity of the (111) faces [henceforth to be referred to as the $(111)_{Zn}$ and the $(111)_{Te}$ face] was done by means of the chemical etch developed by Warekois et al.[12] This method, although perfectly adequate for microscopic identification of the $(111)_{Te}$ and $(111)_{Zn}$ faces, leaves a deposit on the $(111)_{Zn}$ face. This is a disadvantage if the crystal is to be used subsequently as a substrate for film deposition or any optical or electrical work requiring clear crystal surfaces.

In the course of screening various chemical etchants, it was found that chemical polishing of ZnTe with concentrated sodium hydroxide avoids this difficulty. The NaOH solution can be used at its boiling point, in which case a few seconds is adequate to achieve a good polish. It works also at room temperature if times of the order of 10-20 minutes are allowed for the chemical reaction to take place. It is essential that after

the treatment with NaOH the crystal be washed immediately under briskly flowing hot tap water to quickly remove the hydrolysis products of the tellurates which are formed in the reaction of ZnTe with NaOH. The crystals treated by this method are chemically clean and crystallographically relatively perfect. Exciton spectra of ZnTe crystals treated by this method are indistinguishable from exciton spectra obtained from freshly cleaved ZnTe surfaces. Fig. 12 shows the photomicrographs of a ZnTe crystal treated with hot NaOH. Fig. 12A displays the $(111)_{Te}$ face and Fig. 12B the $(111)_{Zn}$ face. The different appearance of the two is quite unmistakable. The $(111)_{Zn}$ and the $(111)_{Te}$ sides of crystals treated by this method can be recognized even without the aid of a microscope. The Te side which contains the large shallow triangular structures is, for all practical purposes, specularly reflecting, while the Zn side has a silvery sheen produced by the many reflections from the sides of the small deep etch pits.

The X-ray and electron diffraction patterns by which the CdS films were identified as single-crystalline and epitaxial with the substrate, were usually taken in spots well away from the crystal edges or any phase or twin boundaries. Visual inspection of crystals containing twins invariably revealed a characteristic striped appearance, with the epitaxial portions of the CdS film shiny, and the non-epitaxial deposits on the misoriented twins matte. The photomicrographs in Fig. 13 show that the transition from epitaxial to non-epitaxial deposition is not sharp but gradual. Fig. 13A is a photomicrograph, under

250 x magnification, of an epitaxial CdS deposit, taken in the middle of a $(111)_{Zn}$ face. One can see rows of regular-shaped growth figures arranged in a shingle-like fashion. Fig. 13B is a photomicrograph of the same crystal showing a twin face and a portion of the $(111)_{Zn}$ face adjacent to the twin. The CdS deposit on the twin is polycrystalline, but one can also see that near the twin boundary the growth figures on the $(111)_{Zn}$ face have become disordered. Evidently the polycrystalline growth which is nucleated on the misoriented twin can push across the twin boundary and interfere to some extent with the single-crystalline overgrowth on the $(111)_{Zn}$ face in the region close to the twin boundary.

4.2 Electrical Properties ZnTe-CdS Diodes

Previous work with ZnTe-CdS heterojunctions[13] had shown that the functional dependence of the forward current on voltage deviated strongly from the behavior predicted from semiconductor theory. More specifically, the log I versus V plots exhibited slopes which were at best about q/5kT, instead of the q/kT or q/2kT, required by theory for a p-n or a p-i-n junction, respectively.

Reproducible fabrication of CdS films which were epitaxial rather than polycrystalline, improved the over-all quality of the diodes by reducing the number of diodes with slopes smaller than $\sim$ q/5kT. Yet, attempts to increase the slope beyond this figure were not successful, indicating that a factor other than the perfection of the CdS film was responsible for the "softness" of the forward characteristic. As it is conceivable that bulk

and surface leakage at low voltages, coupled with series bulk resistance at higher voltages, can combine to produce an apparent logarithmic behavior of the forward I-V characteristic over a limited voltage range, the different junction components were investigated for possible sources of leakage currents and series resistance.

The possible sources of series resistance are the bulk CdS and ZnTe, the external contacts to them, and a possible intrinsic or near-intrinsic layer at the junction. The thickness of the CdS films on the diodes has always been less than approximately 10 microns. Therefore the resistivity of CdS would have to be rather high for it to become the current limiting factor. Yet diodes with CdS resistivities of only a few ohm-cm have often shown quite poor forward characteristics. Bulk ZnTe, being of a thickness of about one mm, can become a current limiting factor when its resistivity exceeds a fewkohm-cm. But, again, diode characteristics could not be improved by going to ZnTe with even as low a resistivity as one ohm-cm. The electrical contacts to the CdS film (fused In) turned out to be quite ohmic, with a negligible contact resistance. The fused In-Ag or evaporated gold electrodes on ZnTe, however, showed a considerable contact resistance.

After testing a number of electrode materials and ZnTe surface treatments, it was found that the contact resistance to ZnTe could be significantly lowered by introducing two modifications in the previous electroding technique. First, the contact to ZnTe was made quite large, about ten times the area of the In contact

to the CdS film, which contact was usually of the order of 10^{-2} cm^2. Second, the In-Ag or evaporated Au electrodes were replaced by either chemically formed Au or Cu_2Te electrodes, in either case with a preceding surface preparation involving chemical polishing with NaOH, and with a backing of In-Ag alloy. Preliminary tests have shown that the contacts prepared by this method have a resistance between 10 and 100 ohms. In a few cases resistances of less than 10 ohms have been achieved.

In order to reduce leakage currents through possible random imperfections in the CdS film, the film was removed from the ZnTe crystal, except for the area directly under the fused In electrode. The resulting geometry of the junction is schematically shown in Fig. 14.

The radical improvement in the forward characteristic produced by these changes is illustrated in Fig. 15. This junction was prepared with chemically deposited Au electrodes to ZnTe. Except for the area under the In electrode, the CdS film was sandblasted off the ZnTe crystal. The log I versus V plot now has a slope of q/2kT over approximately three decades in current. The pre-exponential term, which represents the saturation current, is 9×10^{-10} amp ($\sim 10^{-7}$ amp/cm^2), which is by about one order of magnitude less than that for the junctions prepared by the old technique.*

---

* A large "apparent saturation current", I_o, in $I = I_o (e^{qV/2kT} - 1)$, obtained as the extrapolated intercept of a log I versus V plot, often signifies the presence of leakage. The term "apparent" is used here because the extrapolation of slopes much smaller than q/2kT does not lead to a true saturation current.

After exhibiting a good I-V relationship up to about one volt, the characteristic starts bending over and assumes the shape indicative of a linear I-V relationship beyond about two volts. Such a behavior is clearly indicative of series resistance. While the series resistance in the present case can be due to the bulk resistance of the n-type CdS film (in this particular diode the resistivity of the CdS film was rather high), it is also possible that there exists an intrinsic or near-intrinsic layer between n-type CdS and p-type ZnTe. The existence of such a region is also suggested by the q/2kT slope the log I versus V plot for this diode, which behavior is indicative of either a p-i-n configuration, or a p-n junction in a modulated voltage region. The results of the examination of an angle-lapped junction described below confirms this hypothesis.

4.3 Structure of Angle-Lapped Heterojunctions

The angle-lapping of a ZnTe-CdS diode was accomplished by mounting the ZnTe crystal with the deposited CdS film facing up on a plate-glass slab so that the plane of the CdS film formed an angle of approximately 1^{o} with the plane in which the lapping was to take place. The resulting structure was first ground with medium grade Linde alumina, and finished off with 0.2 μ grain size diamond polish. The exact lap angle was subsequently determined by focussing a high-power microscope at regular intervals along a line perpendicular to the junction on the lapped portions of the diode. The change of focal length per unit distance perpendicular to the junction is then equal to the tangent of the lap angle. By repeated traverses the angle was found to be

1° 10' ± 3'. The exposed portion of the CdS film on the lap plane was measured to be 0.4 mm, giving a film thickness of 0.4 (mm) tan ($1^{\circ}10'$) ≈ 8 μ. This is in satisfactory agreement with the figure of 7 μ, obtained by direct thickness measurements with a precision dial gauge.

It had been observed previously that the CdS films deposited by the technique used in manufacturing the ZnTe-CdS junctions, exhibited a green fluorescence under 3650 Å ultraviolet excitation at room temperature. This is the so-called "edge emission"[14] which is usually observed in unactivated CdS at liquid N_2 temperatures, and occasionally in high purity crystals at room temperature[15]. A contamination of CdS by acceptor impurities like Cu or Ag, inhibits the appearance of the green fluorescence. If present in sufficient concentrations, Ag or Cu produce their own characteristic fluorescence which lie in the red and deep red, respectively. The red and deep red fluorescence can usually be observed at room temperature.

Fig. 16 is a magnified (20x) photograph of an angle-lapped ZnTe-CdS junction taken under ultraviolet excitation. The bright circular shape at the right is the electroded portion of the film. The dark ring around it is the sandblasted area. Below this configuration one can see three or four twins running across the face of the crystal. The luminosity of all these areas is due to the above mentioned green edge emission. The junction is in the middle of the photograph and has a total width (on the photograph) of about 8 mm. In the middle of this 8 mm wide strip is an approximately 4 mm wide streak of dots which are red-luminescent.

The red luminescence appears spotty rather than continuous because of slight pitting during the lapping operation. At the left one can just barely see the outline of the exposed non-luminescent ZnTe.

The presence of the red-luminescent region clearly indicates the existence of an intrinsic or near-intrinsic layer of CdS under the n-type green luminescent exterior. The width of this layer is $\frac{4(\text{mm}) \tan \alpha}{\text{magnification factor}} = 4\ \mu$. As CdS films deposited by the same technique on quartz slides are green-luminescent all the way through, the appearance of the red-luminescent layer in CdS films deposited on ZnTe must be associated with either mixed crystal formation between ZnTe and CdS, or the diffusion of Cu or Ag from ZnTe into CdS. Although some mixed crystal formation cannot be ruled out, it is not very probable, as CdS and ZnTe tend to undergo a metathetical reaction leading to ZnS and CdTe. On the other hand, since the ZnTe crystal used in this study was Cu-doped, and Cu is a fast diffuser in II-VI compounds, the diffusion of Cu from ZnTe into CdS during film formation is quite likely. It will be assumed, therefore, that the red-luminescent region in CdS is due to Cu luminescence centers formed by Cu originating from ZnTe.

Such a rearrangement of dopants in junctions is undesirable not only because of the formation of intrinsic or near-intrinsic layers in the CdS film, but also because it depletes the ZnTe of its acceptor centers in the vicinity of the junction. There is, fortunately, a way to overcome this difficulty. It was shown in Section 3.4 that Zn vacancies can act as acceptor centers in ZnTe, and that the room temperature carrier concentration in the self-doped

crystals can be as high or higher than in the Cu-doped crystals. The room temperature hole concentration of self-doped ZnTe 1286 (of Fig. 11), for example, is 8×10^{16} cm^{-3}, while the Cu-doped ZnTe 113 has a hole concentration of 6×10^{16} cm^{-3}.

The rectifier characteristic of a diode prepared by depositing CdS on self-doped ZnTe is shown in Fig. 17. The log I versus V slope of the forward characteristic is somewhat inferior and the rectification ratio somewhat better than that of Diode 21 (Fig. 15). It is noteworthy, however, that the characteristic in Fig. 17 was obtained with a junction in which the film area under the In contact was not isolated from the rest of the film as in Diode 21. This shows that such a treatment is not a necessary condition for obtaining good forward characteristics. An angle-lap of this junction showed that the red-luminescent region in the CdS film was again present, in spite of the fact that the ZnTe crystal was not intentionally Cu-doped. This is, perhaps, not surprising because of the presence of Cu as an impurity in many "undoped" ZnTe crystals (cf. crystal ZnTe 117, Section 3.4). It is intended, therefore, to prepare future diodes from ZnTe crystals which have been treated with liquid Zn to reduce in them the concentration of the Cu impurity.

5. PLANS FOR THE NEXT REPORTING PERIOD

In the CdS work, the emphasis will be on using equipment now being built to permit the study of intrinsic CdS at as low a temperature as 100°C and then study the effects of additions of Ag. Provisions for possible optical excitation of holes have been made.

The transport measurements as well as the investigation of the energy level structure of ZnSe and ZnTe will be continued, with emphasis on attempts to resolve the sited discrepancies between experiment and theory.

In the area of ZnTe-CdS heterojunctions, attempts will be made to prepare junctions without the compensated layer between ZnTe and CdS. Work will be continued in investigating the exact sources of series resistance and leakage in the manufactured diodes, and finding ways to minimize them.

6. ACKNOWLEDGEMENTS

It is a pleasure to acknowledge helpful conversations with Drs. W. C. Dash, R. E. Halsted and D. A. Cusano. The authors are particularly indebted to Dr. B. Segall for assistance in theoretical interpretation of the experimental results.

7. CONTRIBUTORS

The work described in the preceding report was carried out by:

Staff Members	Technicians
M. Aven	S. J. Polich
H. H. Woodbury	W. Garwacki

8. PAPERS PUBLISHED OR PRESENTED

None

REFERENCES

1. M. Avinor, Thesis, Univ. of Amsterdam, 1959 (p.37).
2. M. Avinor, Thesis, Univ. of Amsterdam, 1959;
   M. Avinor, J. Electrochemical Soc. 107, 608 (1960).
3. M. Aven, D. T. F. Marple and B. Segall, J. Appl. Phys. 32, 2261 (1961).
4. D. J. Howarth and E. H. Sondheimer, Proc. Roy. Soc. A219, 53 (1953).
5. H. Ehrenreich, J. Phys. Chem. Solids 8, 134 (1959).
6. L. R. Shiozawa, S. Devlin and J. M. Jost, 4th Quart. Rept. WADD Contract AF 33(616-6865), Jan. 1961.
7. R. E. Bube and E. L. Lind, Phys. Rev. 110, 1040 (1958).
8. Burstein, Bell, Davidson and Lax, J. Phys. Chem. 57, 849 (1953).
9. W. W. Piper and R. E. Halsted, Proc. Int. Conf. Semicond. Phys., Prague 1960. Publ. House of Czech. Acad. Sci., Prague, p.1046.
10. W. W. Piper and D. T. F. Marple, J. Appl. Phys. 32, 2237 (1961).
11. N. B. Hannay, "Semiconductors", Reinhold Publ. Corp., New York, 1959, p. 30.
12. Warekois, Lavine, Mariano and Gatos, J. Appl. Phys. (in press)
13. M. Aven and D. M. Cook, J. Appl. Phys. 32, 960 (1961).
14. F. A. Kroger and H. J. G. Meijer, Physica 20, 1149 (1954).
15. Y. T. Sihvonen, D. R. Boyd and C. D. Woelke, Phys. Rev. 113, 965 (1959).

FIGURE CAPTIONS

Fig. 1. Transmitted light microphotographs of thin sections of CdS heavily doped with Cu.

Fig. 2. Schematic indication of possible positions for the thermal acceptor levels of the group 1B elements in CdS at 77°K.

Fig. 3. Temperature dependence of mobility for ZnSe.

Fig. 4. Temperature dependence of mobility for ZnTe.

Fig. 5. Temperature dependence of the Hall coefficient for ZnSe 3.

Fig. 6. Temperature dependence of the Hall coefficient and the resistivity for ZnSe 5.

Fig. 7. Temperature dependence of the Hall coefficient and the resistivity for ZnSe 4.

Fig. 8. Temperature dependence of the free hole concentration in ZnTe 117.

Fig. 9. Temperature dependence of the Hall coefficient and the resistivity for ZnTe 113.

Fig. 10. Effect of liquid Zn firing on the temperature dependence of the Hall coefficient of ZnTe 117.

Fig. 11. Effect of the change in Zn vacancy concentration on the temperature dependence of the Hall coefficient of ZnTe 1262, ZnTe 1286 and ZnTe 1287.

Fig. 12. Photomicrographs (250x) of a ZnTe crystal treated with NaOH. A- $(111)_{Te}$ face. B- $(111)_{Zn}$ face.

FIGURE CAPTIONS (Cont.)

Fig.13. Photomicrographs (250x) of CdS deposits on ZnTe.
A- epitaxial deposit on $(111)_{Zn}$ face.
B- degeneration of the epitaxial deposit near a misoriented twin.

Fig.14. Structure of a ZnTe-CdS heterojunction with the new electrode configuration.

Fig.15. Current - voltage relationship for ZnTe-CdS heterojunction diode 21.

Fig.16. Angle-lapped ZnTe-CdS diode under ultraviolet excitation.

Fig.17. Current - voltage relationship for ZnTe-CdS heterojunction diode 25.

A

B

Fig. 1

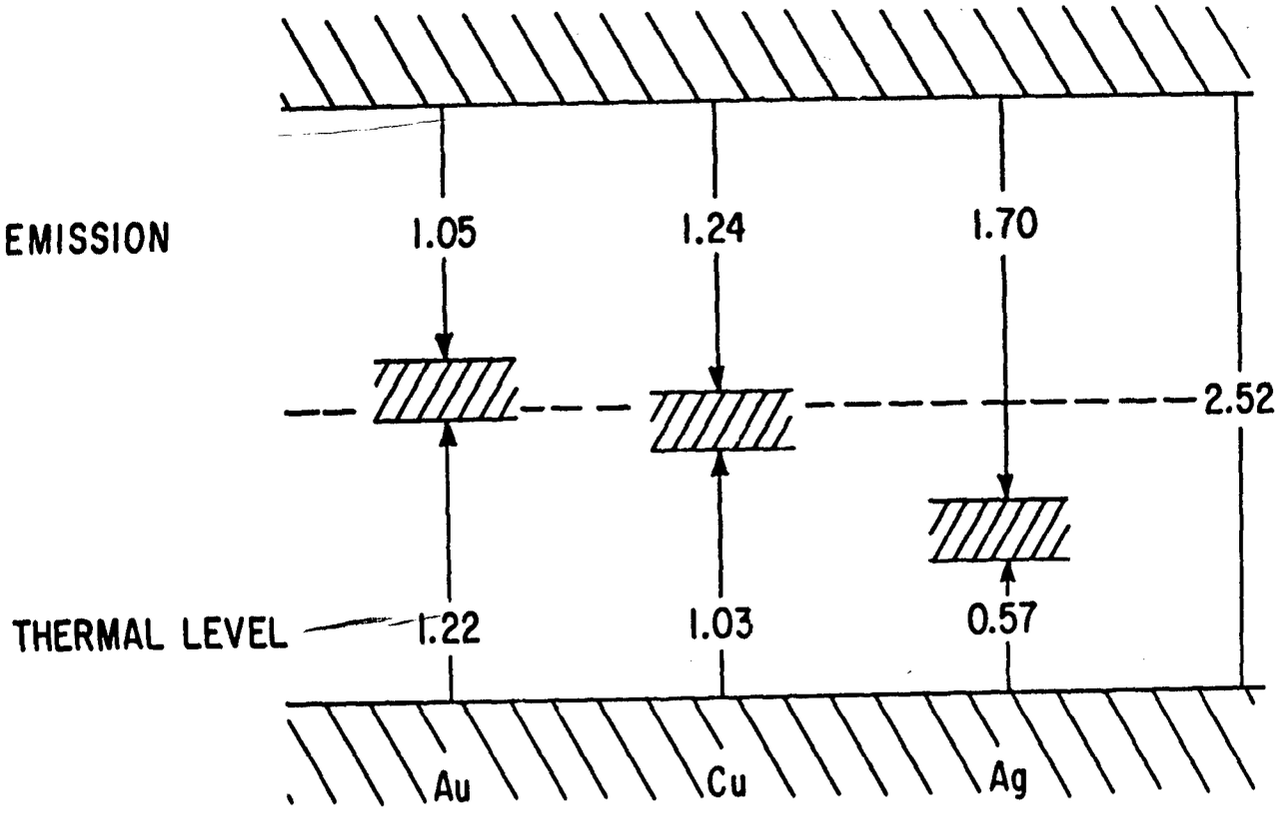

Fig. 2

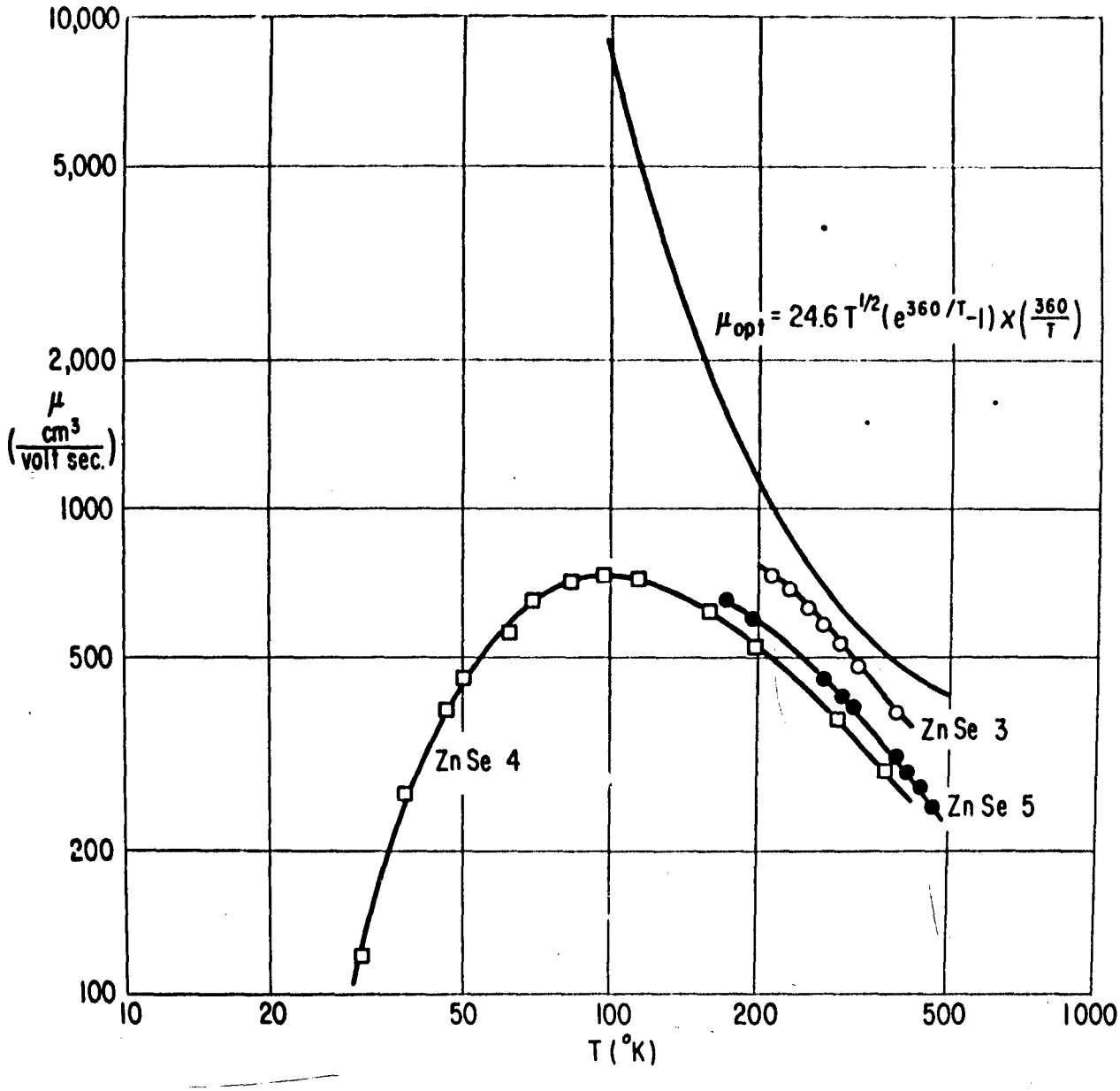
10,000
5,000
2,000
1000
500
200
100
μ (cm³ / volt sec.)
10
20
50
100
200
500
1000
T (°K)
μopt = 24.6 T^1/2 (e^360/T − 1) x (360/T)
Zn Se 4
Zn Se 3
Zn Se 5

Fig. 3

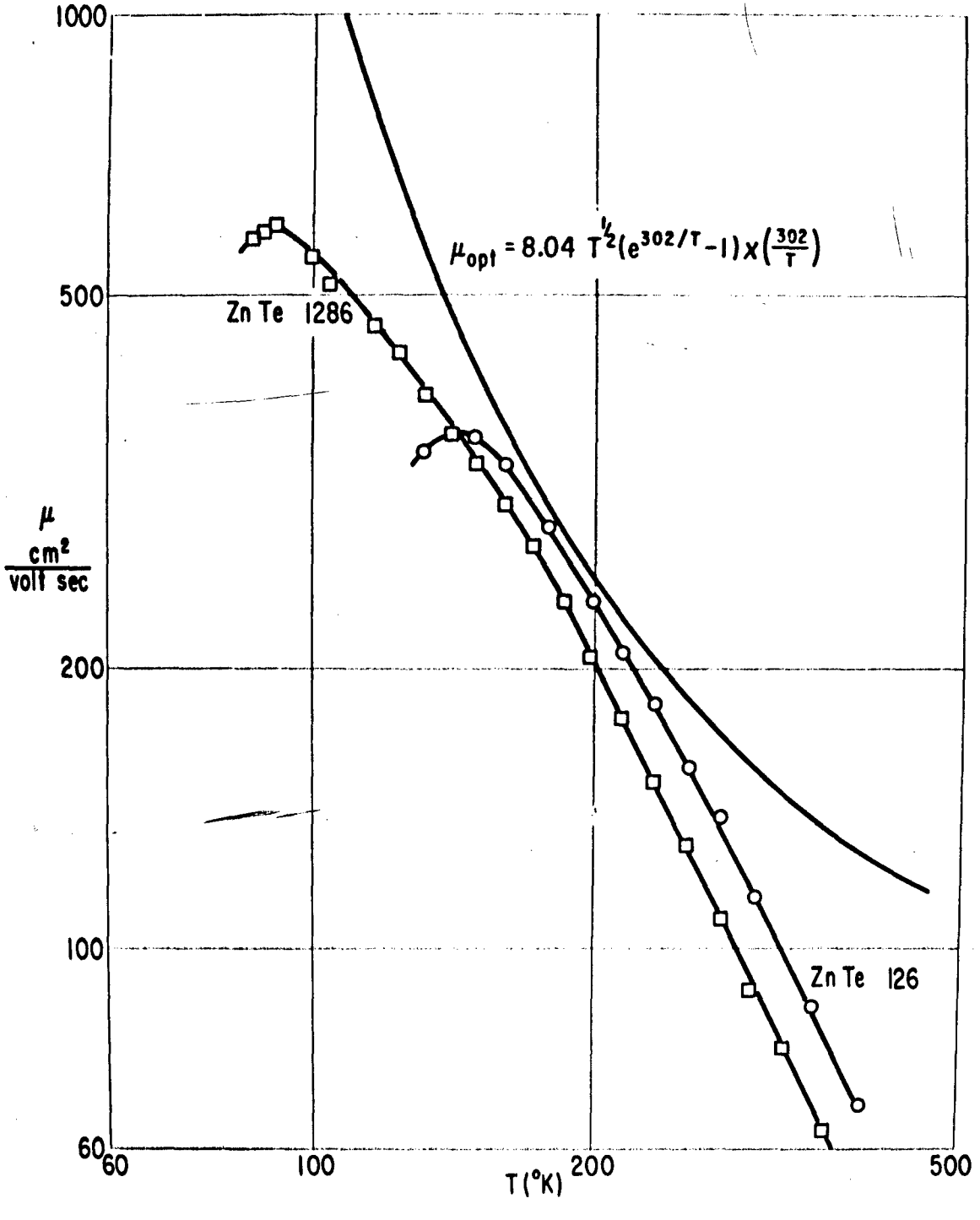
1000
500
200
100
60
60
100
200
500
T(°K)
μ
cm²
volt sec
$\mu_{opt} = 8.04\ T^{1/2}(e^{302/T}-1)\times\left(\frac{302}{T}\right)$
Zn Te 1286
Zn Te 126

Fig. 4

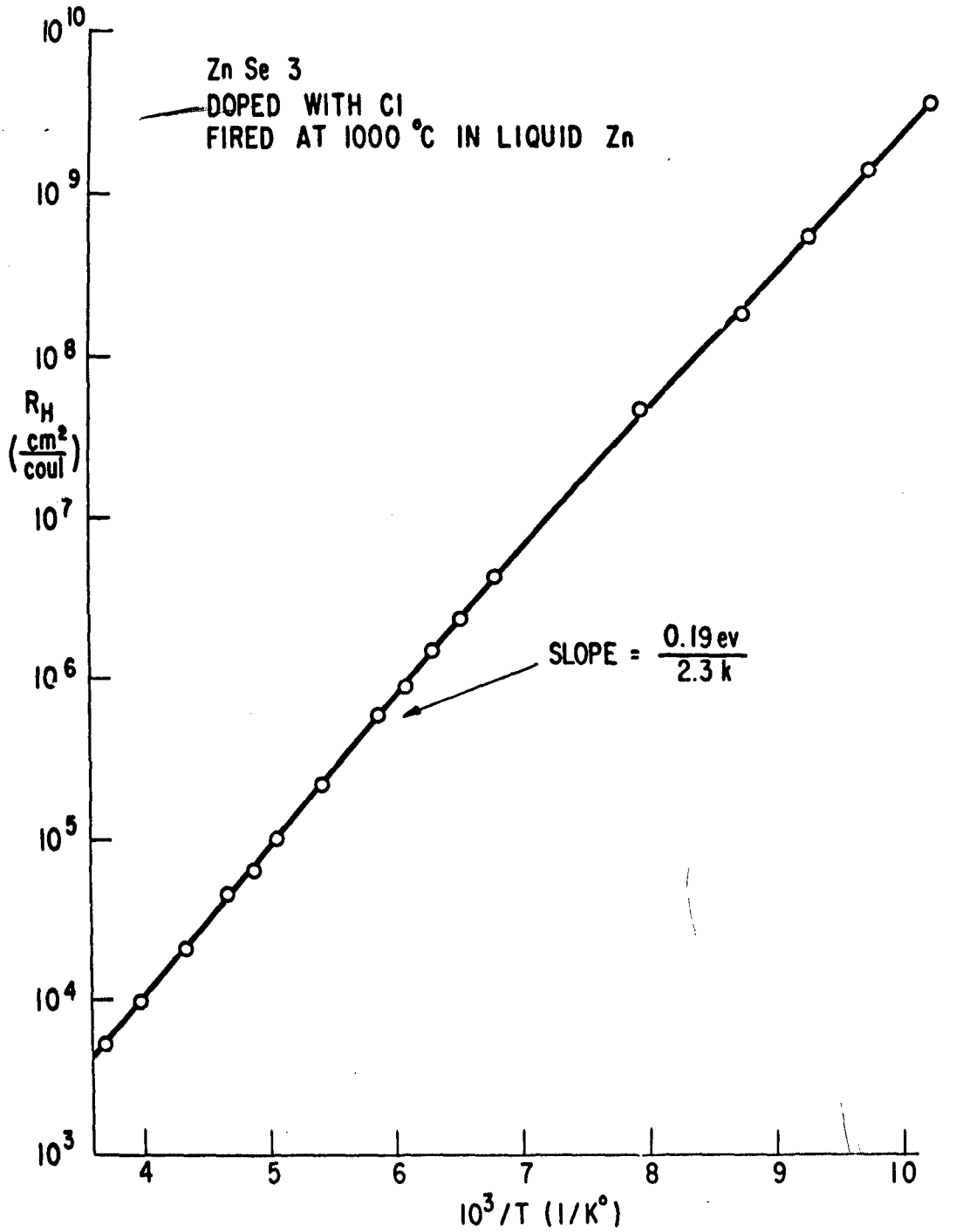
Zn Se 3
DOPED WITH Cl
FIRED AT 1000 °C IN LIQUID Zn
10^{10}
10^{9}
10^{8}
10^{7}
10^{6}
10^{5}
10^{4}
10^{3}
R_H ($\frac{cm^2}{coul}$)
SLOPE = $\frac{0.19\,ev}{2.3\,k}$
4
5
6
7
8
9
10
$10^3/T$ (1/K°)

Fig. 5

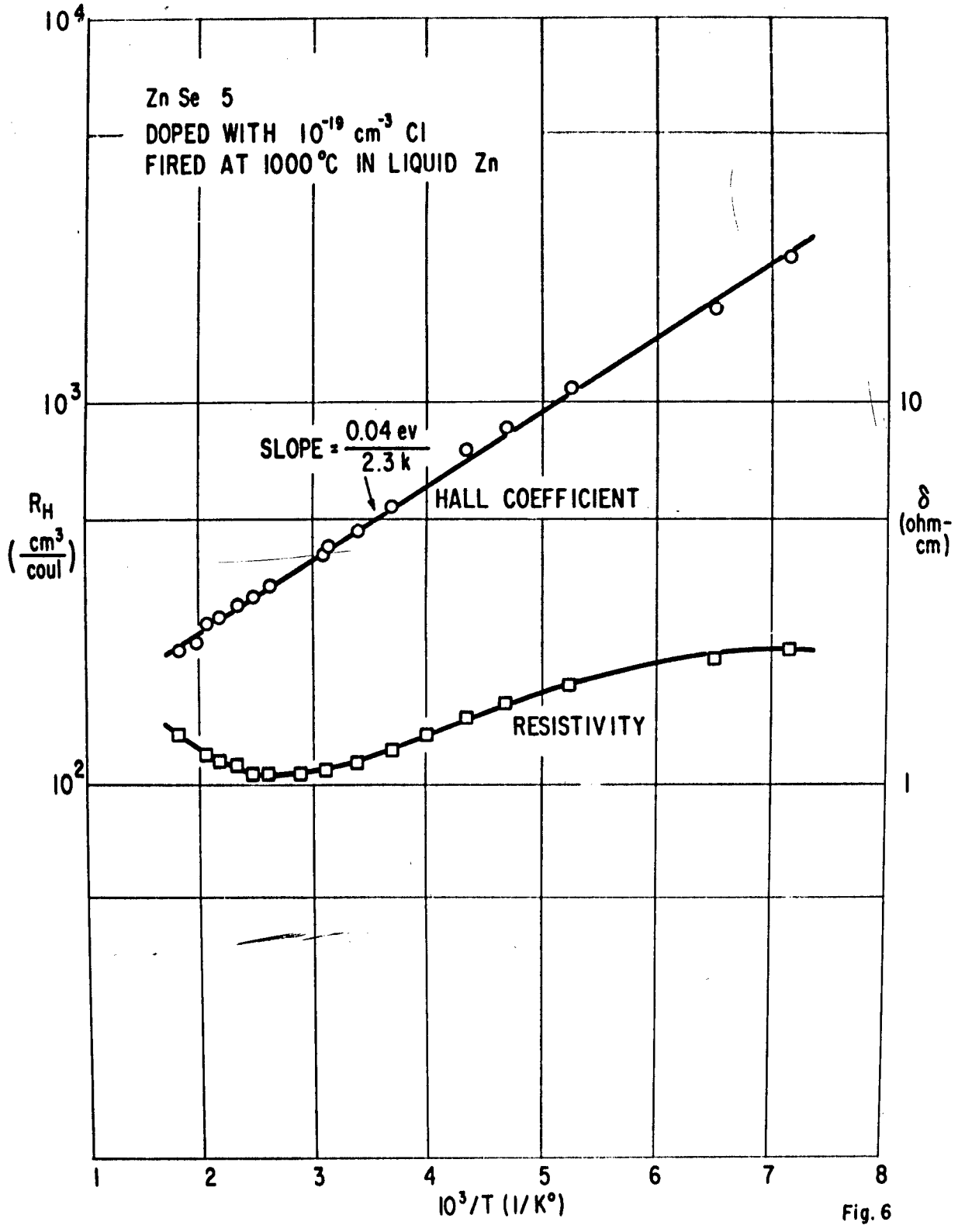
Zn Se 5
DOPED WITH 10^{-19} cm^{-3} Cl
FIRED AT 1000°C IN LIQUID Zn
10^4
10^3
10^2
SLOPE = 0.04 ev / 2.3 k
HALL COEFFICIENT
RESISTIVITY
R_H ($\frac{cm^3}{coul}$)
δ (ohm-cm)
10
1
1
2
3
4
5
6
7
8
$10^3/T$ (1/K°)

Fig. 6

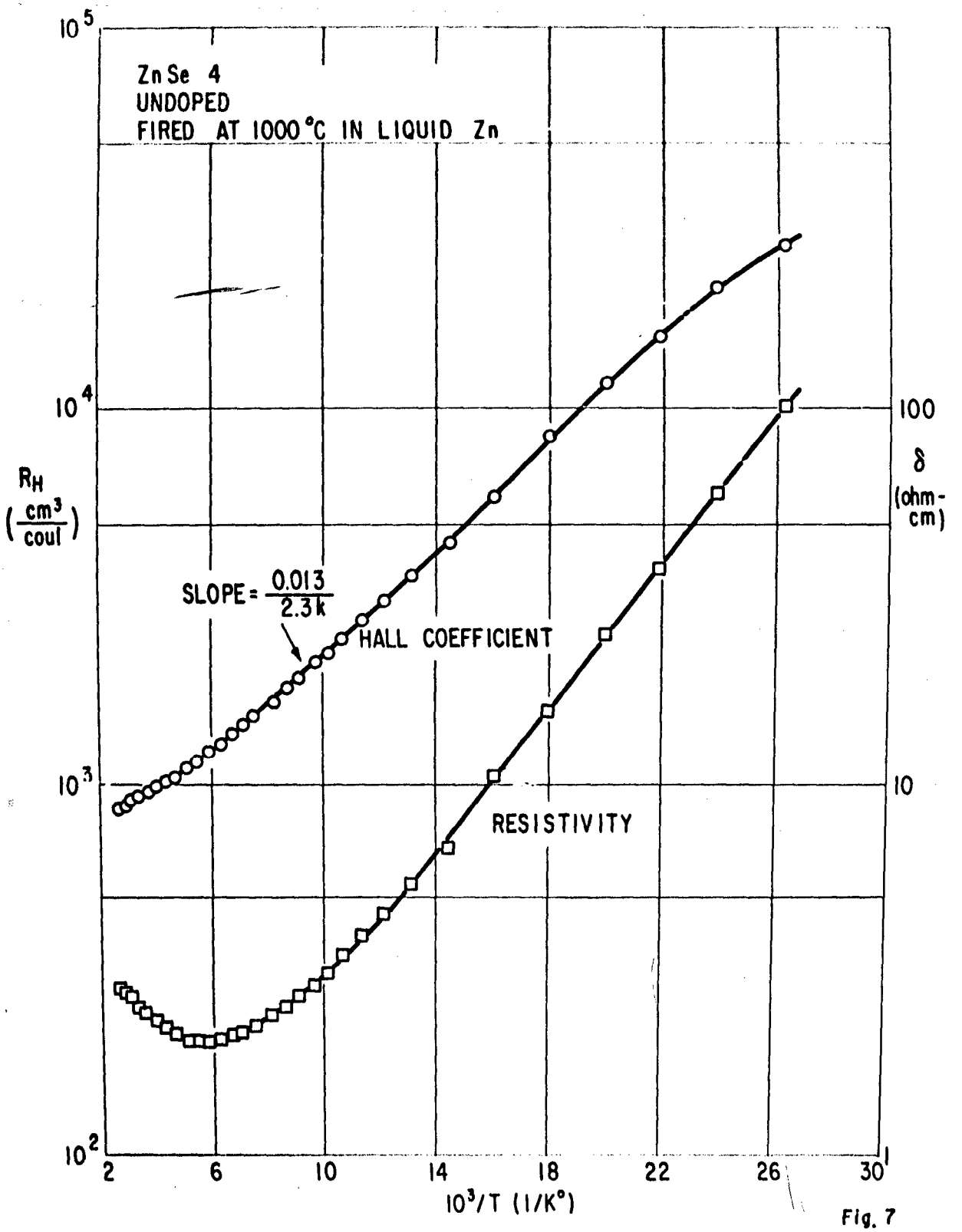
ZnSe 4
UNDOPED
FIRED AT 1000°C IN LIQUID Zn
10^5
10^4
10^3
10^2
R_H ($\frac{cm^3}{coul}$)
SLOPE = $\frac{0.013}{2.3k}$
HALL COEFFICIENT
RESISTIVITY
100
10
δ (ohm-cm)
2
6
10
14
18
22
26
30
$10^3/T$ (1/K°)

Fig. 7

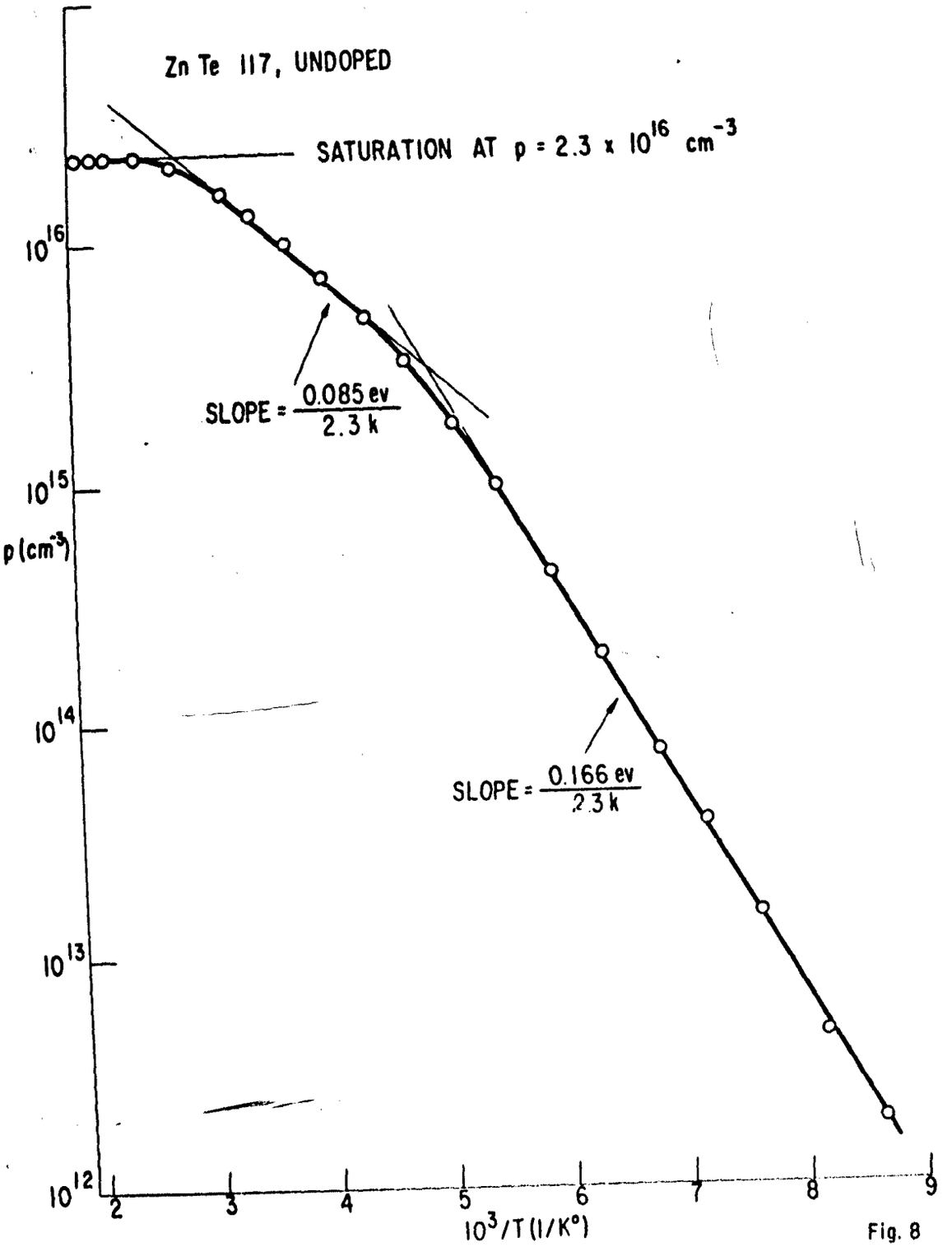
Zn Te 117, UNDOPED
SATURATION AT p = 2.3 x 10^16 cm^-3
SLOPE = 0.085 ev / 2.3 k
SLOPE = 0.166 ev / 2.3 k
p (cm^-3)
10^16
10^15
10^14
10^13
10^12
2
3
4
5
6
7
8
9
10^3/T (1/K°)

Fig. 8

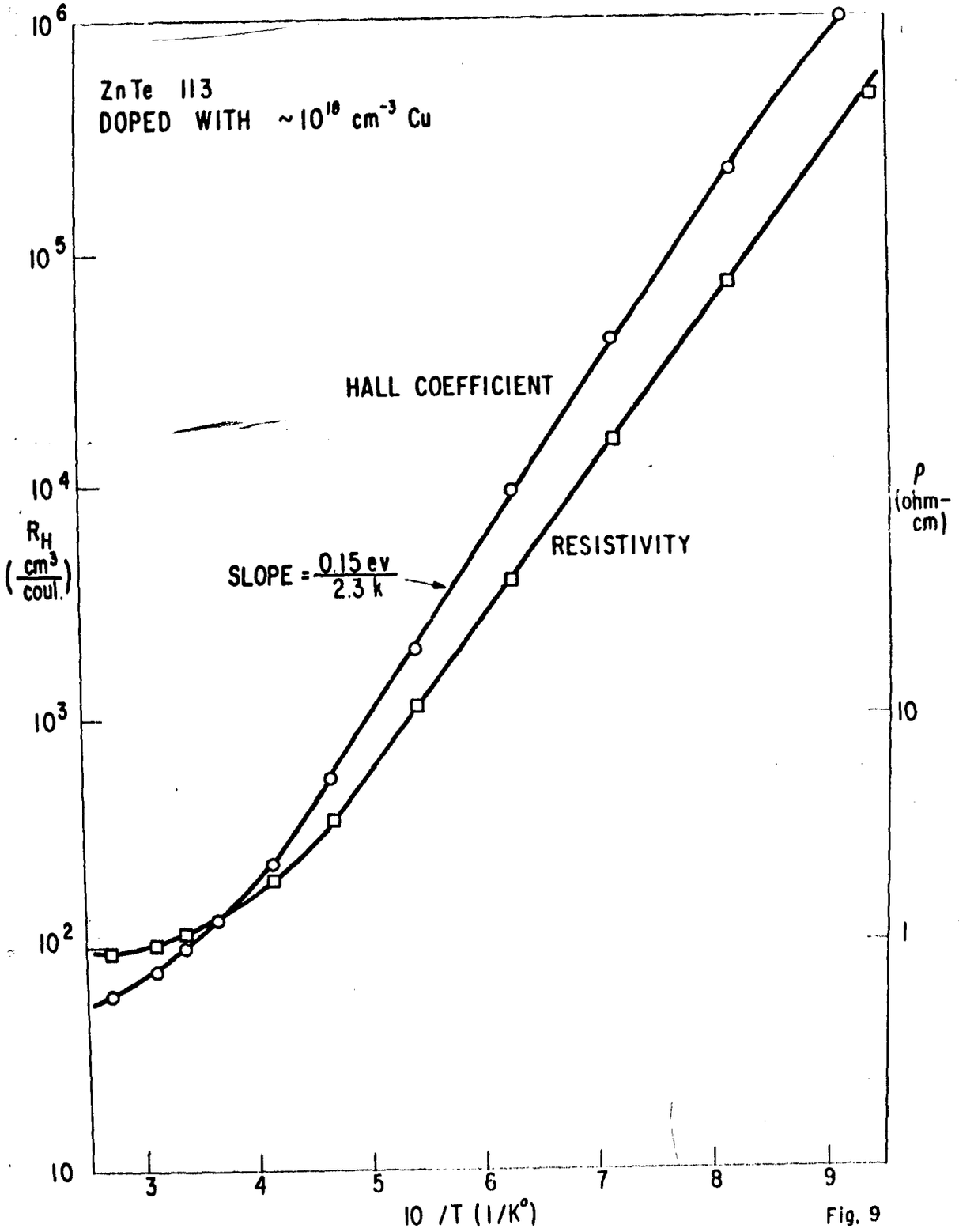
ZnTe 113
DOPED WITH ~10^18 cm^-3 Cu
HALL COEFFICIENT
RESISTIVITY
SLOPE = 0.15 ev / 2.3 k
R_H (cm^3/coul.)
ρ (ohm-cm)
10^6
10^5
10^4
10^3
10^2
10
1
10
10 /T (1/K°)

Fig. 9

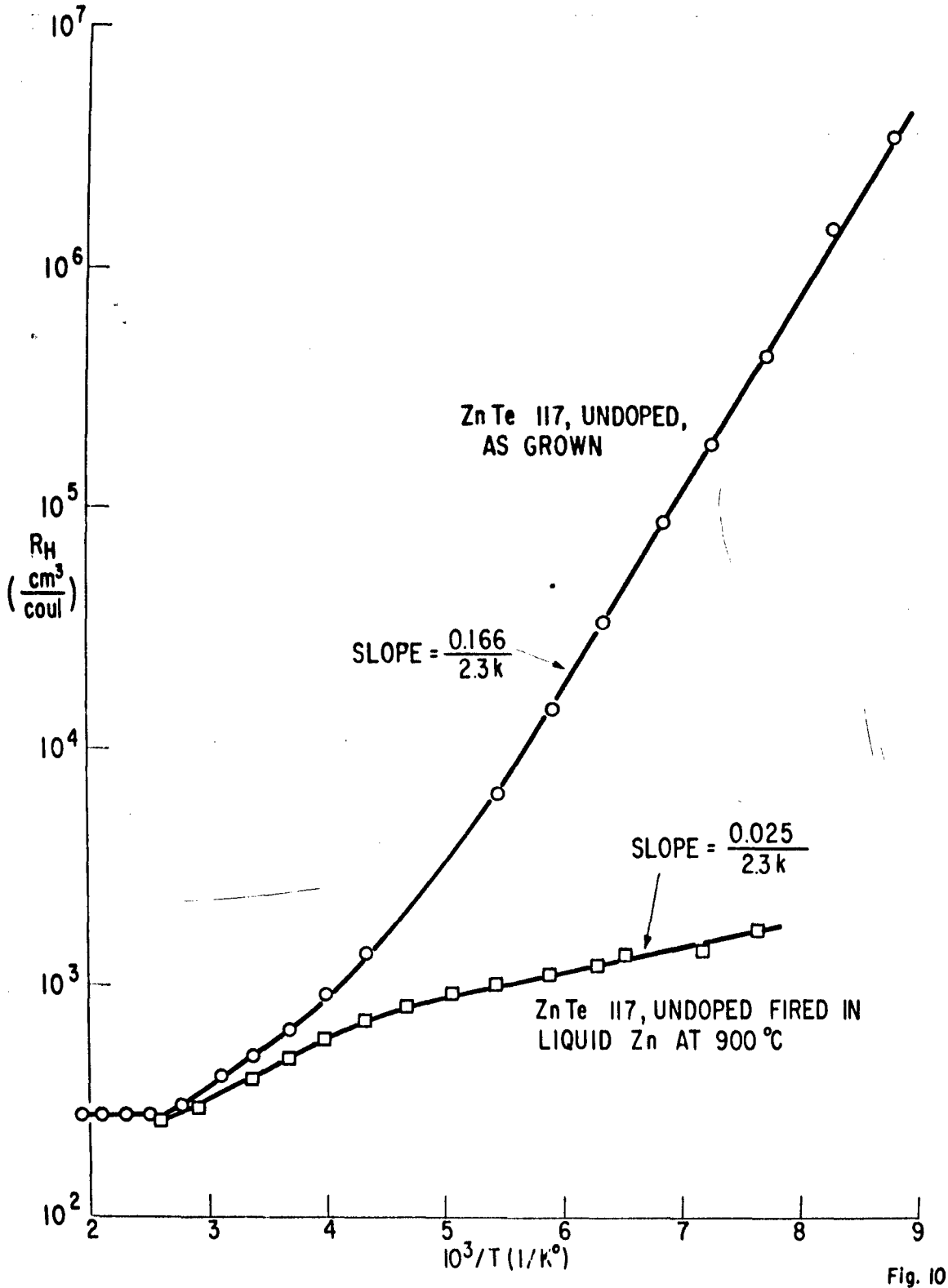
10^7
10^6
10^5
10^4
10^3
10^2
R_H $(\frac{cm^3}{coul})$
Zn Te 117, UNDOPED, AS GROWN
SLOPE = $\frac{0.166}{2.3k}$
SLOPE = $\frac{0.025}{2.3k}$
Zn Te 117, UNDOPED FIRED IN LIQUID Zn AT 900 °C
2
3
4
5
6
7
8
9
$10^3/T$ (1/K°)

Fig. 10

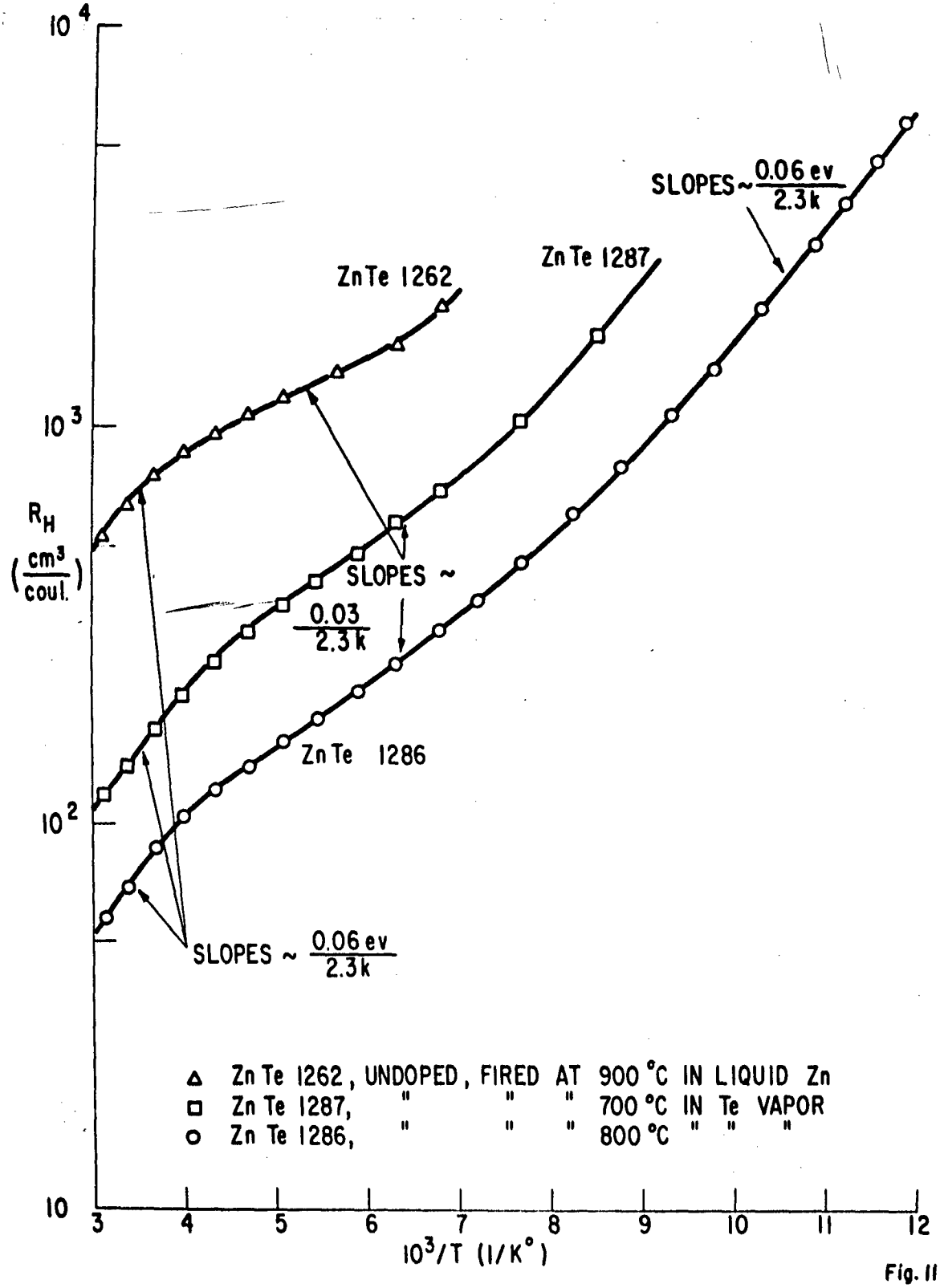
10^4
10^3
10^2
10
R_H ($\frac{cm^3}{coul.}$)
SLOPES ~ $\frac{0.06\,ev}{2.3k}$
ZnTe 1262
ZnTe 1287
ZnTe 1286
SLOPES ~ $\frac{0.03}{2.3k}$
SLOPES ~ $\frac{0.06\,ev}{2.3k}$
△ ZnTe 1262, UNDOPED, FIRED AT 900 °C IN LIQUID Zn
□ ZnTe 1287, " " " 700 °C IN Te VAPOR
○ ZnTe 1286, " " " 800 °C " " "
3 4 5 6 7 8 9 10 11 12
$10^3/T$ (1/K°)

Fig. 11

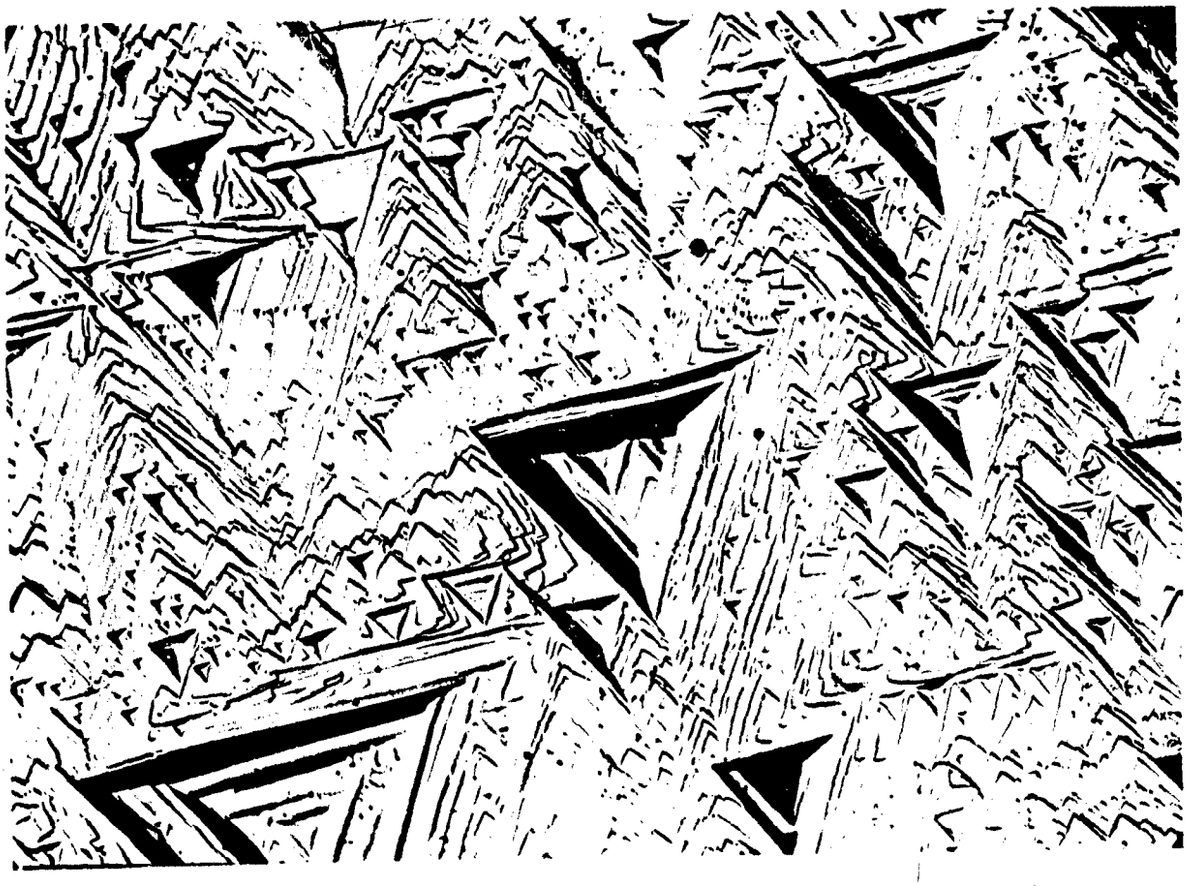

A

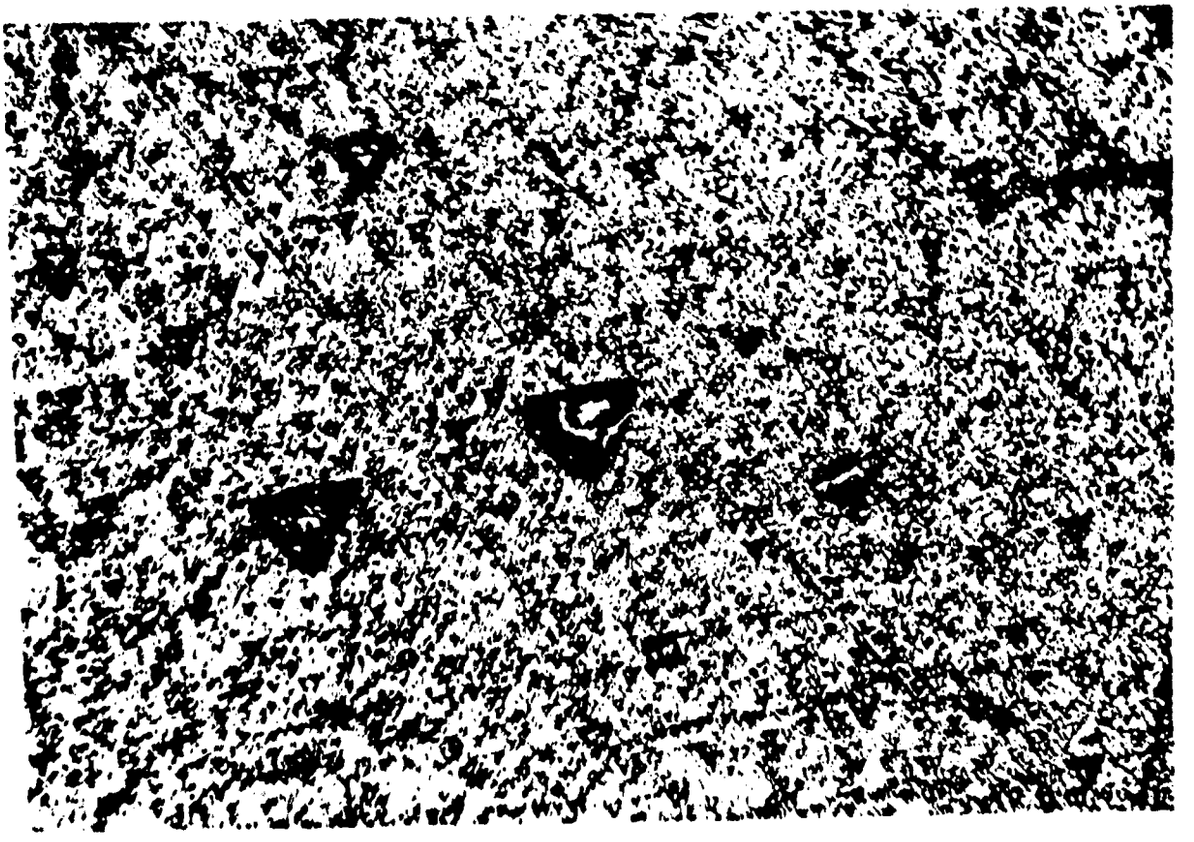

B

Fig. 12

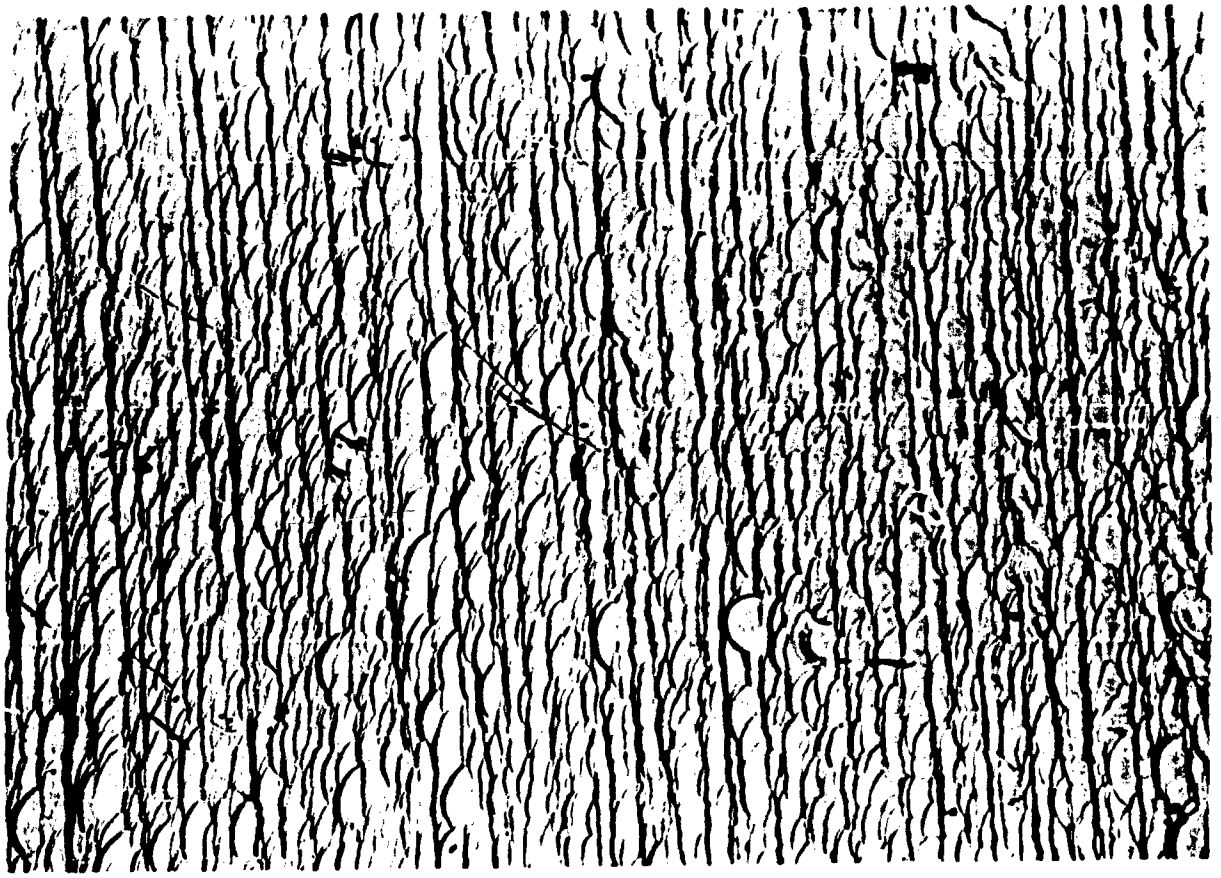

A

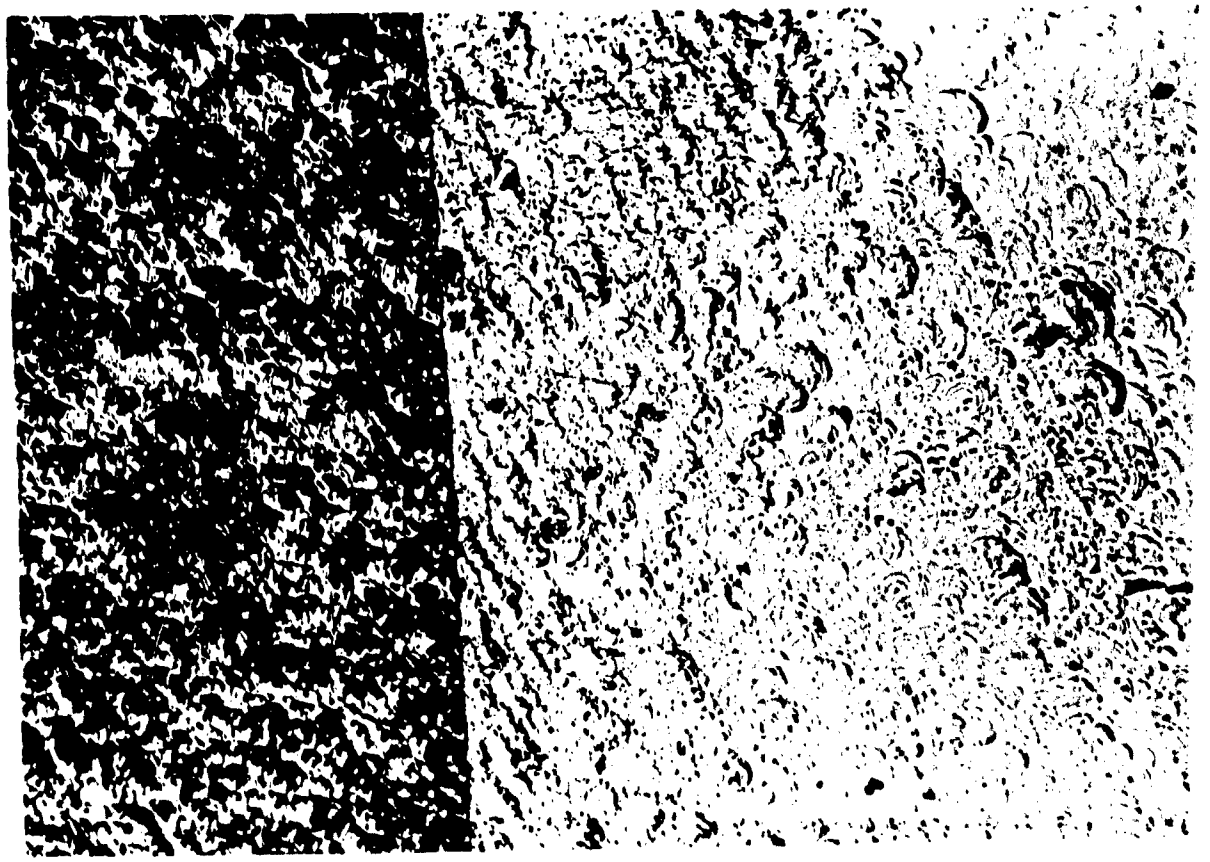

B

Fig. 13

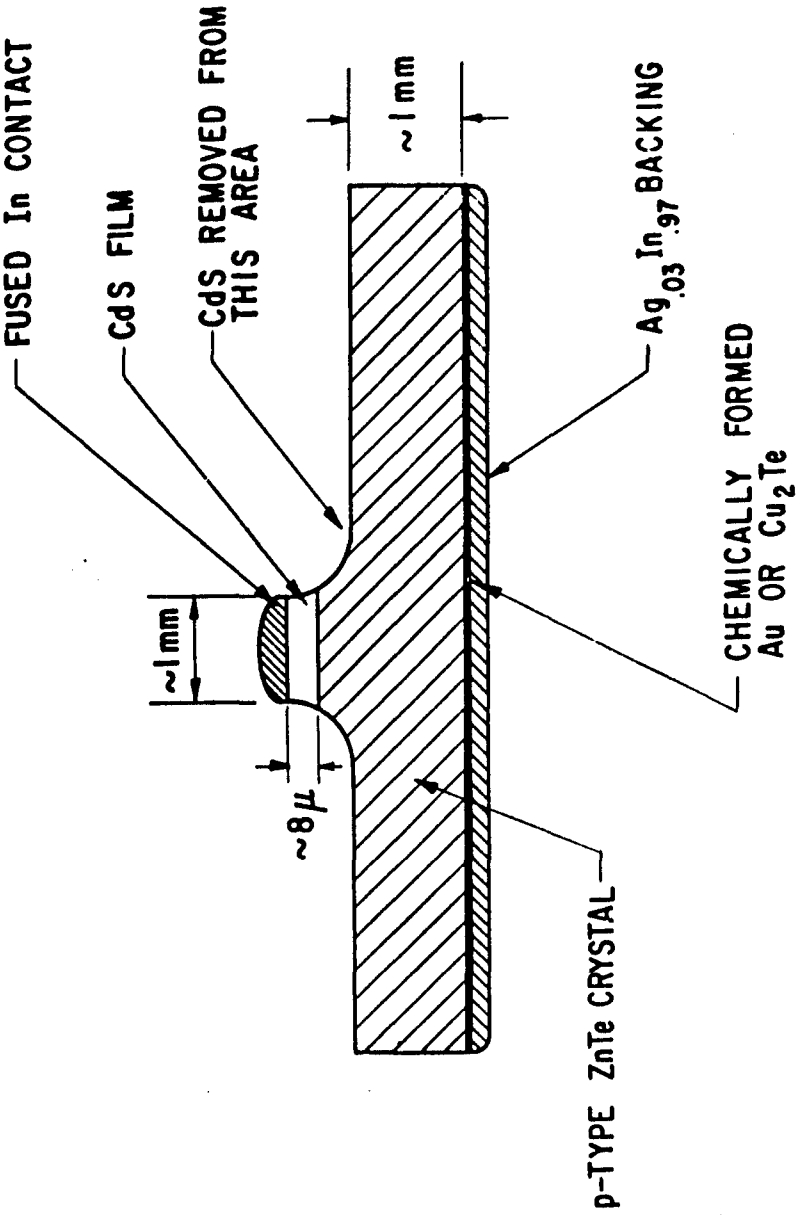
FUSED In CONTACT
CdS FILM
CdS REMOVED FROM THIS AREA
~1mm
~1mm
$Ag_{.03}In_{.97}$ BACKING
CHEMICALLY FORMED Au OR Cu_2Te
~8μ
p-TYPE ZnTe CRYSTAL

Fig. 14

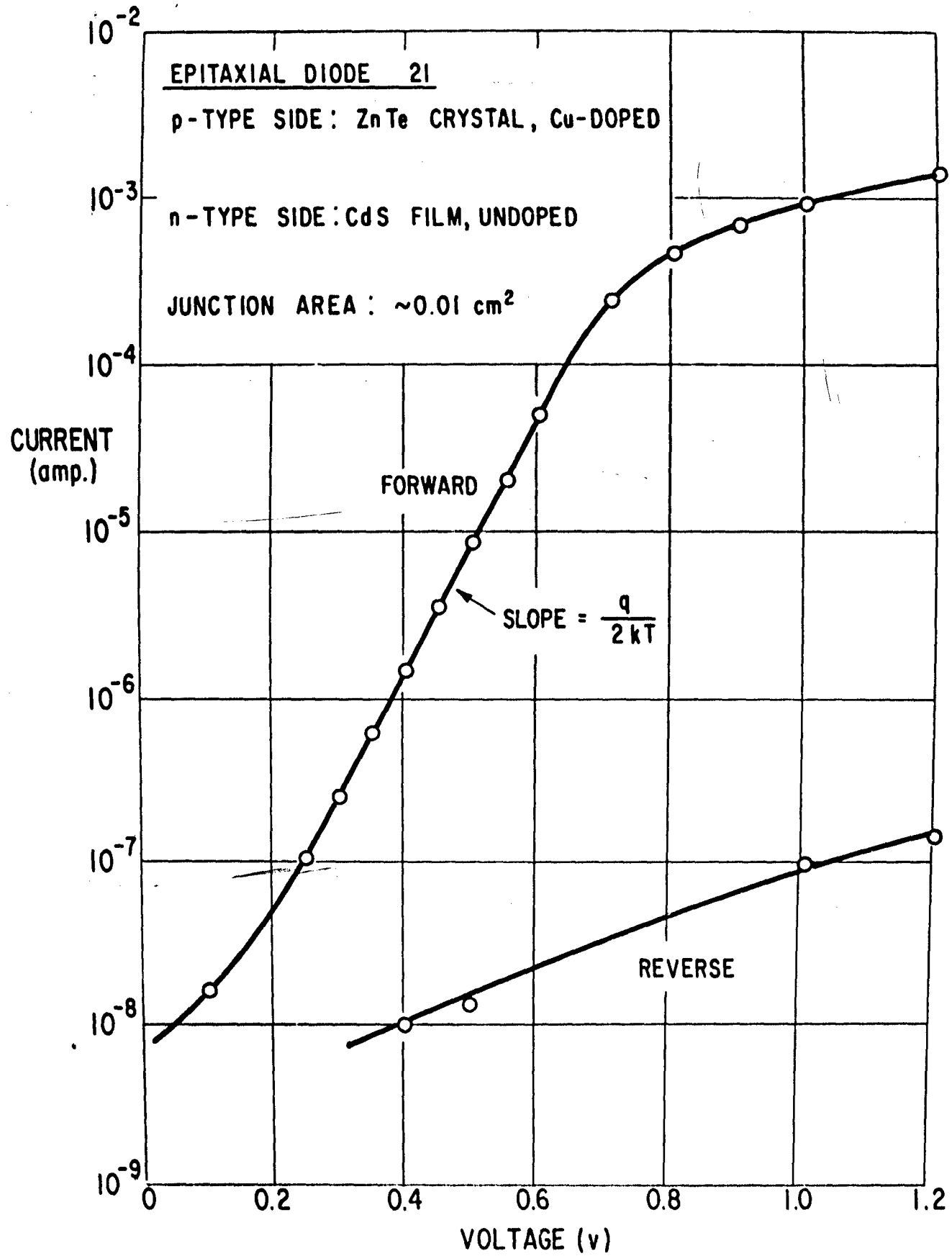
EPITAXIAL DIODE 21
p-TYPE SIDE: ZnTe CRYSTAL, Cu-DOPED
n-TYPE SIDE: CdS FILM, UNDOPED
JUNCTION AREA: ~0.01 cm²
CURRENT (amp.)
FORWARD
SLOPE = q/2kT
REVERSE
VOLTAGE (v)
10⁻²
10⁻³
10⁻⁴
10⁻⁵
10⁻⁶
10⁻⁷
10⁻⁸
10⁻⁹
0
0.2
0.4
0.6
0.8
1.0
1.2

Fig. 15


TOTAL WIDTH OF
JUNCTION 8μ
4μ
WIDTH OF RED-LUMINESCENT
LAYER

Fig. 16

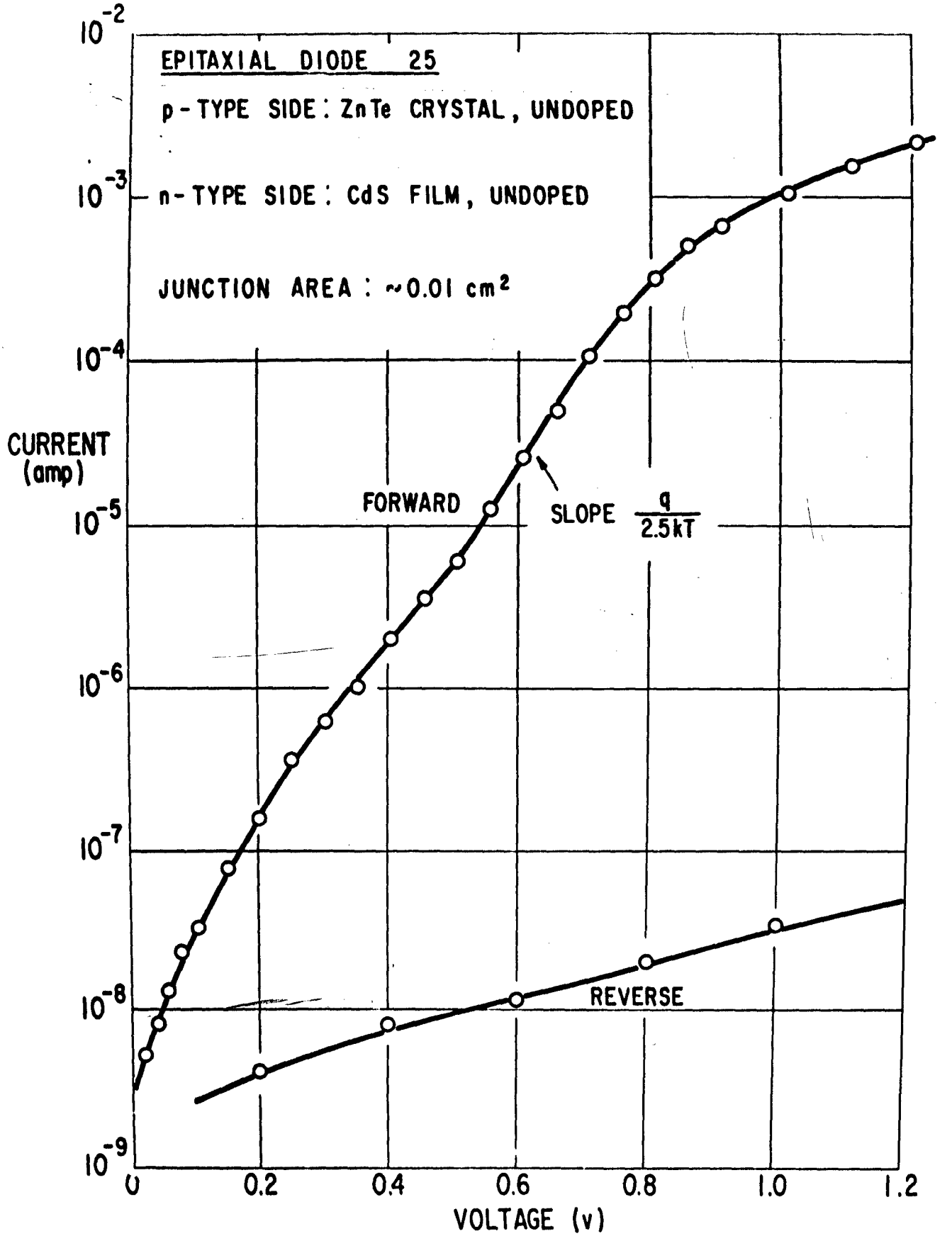
EPITAXIAL DIODE 25
p-TYPE SIDE: ZnTe CRYSTAL, UNDOPED
n-TYPE SIDE: CdS FILM, UNDOPED
JUNCTION AREA: ~0.01 cm²
CURRENT (amp)
FORWARD
SLOPE q/2.5kT
REVERSE
VOLTAGE (v)
10⁻²
10⁻³
10⁻⁴
10⁻⁵
10⁻⁶
10⁻⁷
10⁻⁸
10⁻⁹
0
0.2
0.4
0.6
0.8
1.0
1.2

Fig. 17